2013

Skein theory and topological quantum field theory

Xuanting Cai
Louisiana State University and Agricultural and Mechanical College, xcai1@math.lsu.edu

SKEIN THEORY AND TOPOLOGICAL QUANTUM FIELD THEORY

A Dissertation

Submitted to the Graduate Faculty of the
Louisiana State University and
Agricultural and Mechanical College
in partial fulfillment of the
requirements for the degree of
Doctor of Philosophy

in

The Department of Mathematics

by
Xuanting Cai
B.S., Peking University, 2007
M.S, Louisiana State University, 2008
May 2013

Acknowledgements

This dissertation would not be possible without several contributions. First of all, I am extremely grateful to my advisor, Prof. Gilmer, for his constant encouragement and guidance throughout this work.

Meanwhile, I really wish to express my sincere thanks to all the committee members, Prof. Dasbach, Prof. Litherland, Prof. Richardson, Prof. Sage and the Dean's representative Prof. Thomas Ricks, for their help and suggestions on the corrections of this dissertation.

I also take this opportunity to thank the Mathematics department of Louisiana State University for providing me with a pleasant working environment and all the necessary facilities.

This dissertation is dedicated to my parents and my wife for their unceasing support and encouragement.

Table of Contents

Abstract

Skein modules arise naturally when mathematicians try to generalize the Jones polynomial of knots. In the first part of this work, we study properties of skein modules. The Temperley-Lieb algebra and some of its generalizations are skein modules. We construct a bases for these skein modules. With this basis, we are able to compute some gram determinants of bilinear forms on these skein modules. Also we use this basis to prove that the Mahler measures of colored Jones polynomial of a sequence of knots converges to the Mahler measure of some two variable polynomial.

The topological quantum field theory constructed by Blanchet, Habegger, Masbaum and Vogel can be considered as a generalization of quantum invariants. It assigns modules to surfaces and linear maps to cobordisms. In particular, it assigns the ground ring to empty surface and constants to cobordisms of empty surface to itself, which are closed 3-manifolds. In this way, we get quantum invariants of 3-manifolds back. In the second part of the work, knot invariants are constructed using topological quantum field theory from quantum invariants of tangles. We prove that this is another way to compute the Turaev-Viro polynomial of knots and related invariants.

Chapter 1
Introduction

The notation of skein relations was introduced by Conway in his study of Alexander polynomial [Co]. However, the skein theory was fully developed after the appearance of Kauffman bracket [Ka1], which give an elegant way to define Jones polynomial combinatorially. After that, Turaev and Przytycki define skein modules using Kauffman bracket, which are generalizations of the space of Jones polynomials. Skein modules are used in various places, for example, construction of quantum invariants [Li1, Li2, Li3, Li4, Li5], topological quantum field theory [BHMV2] and more recently AJ-conjecture [BP, FGL, L, G]. In this thesis, we first study properties of some special skein modules.

In Chapter 2, we concentrate on the Temperley-Lieb algebra, which is the skein module of $I \times I$ with $2n$ points on the bounday. We investigate the algebraic structure of the Temperley-Lieb aglebra as a module. Based on theory in [KL] and [BHMV2], we construct an orthogonal basis for the Temperley-Lieb algebra, which is the Schmidt's orthogonalization of a well-known natural basis of it. We show that this basis after normalization is the same as the basis constructed in [DiF], but constructed in a simpler way. Then we study the bilinear form on the Temperley-Lieb algebra defined in [Li5]. With this basis, we compute the determinant of this bilinear form with respect to the natural basis. This gives a short proof of the result in [DiF]. This chapter is based on the published paper [Cai].

In Chapter 3, we look at a slight generalization of the Temperley-Lieb algebra, which is still the skein module of $I \times I$ but with $n + 1$ points on boundary and 1 point colored. Using the same technique as in Chpater 2, we construct a basis for this skein module. The reason we are interested in this skein module related to a semi-meander problem that is studied in [DGG, DiF]. We also generalize the bilinear form on the Temperley-Lieb algebra to this module and compute the gram determinant of this bilinear form, which is similar to the semi-meander determinant. The computation is reduced to a combinatorial problem, which is proved in an algebraic method and a geometric method. This chapter is based on the published paper [CM].

In Chapter 4, we focus on the colored Jones polynomial analogue of the Temperley-Lieb algebra, the generalized Temperley-Lieb algebra or the colored Temperley-Lieb algebra. It is a skein module of $I \times I$ with $2n$ points on the boundary with each point colored the same color. In this skein module, we show that some elements in a basis constructed in the same way as last two chapters are idempotents. In [CK], it is shown that the Mahler measure of the colored Jones polynomial of a certain sequence of knots converges to the Mahler measure of some 2-variable polynomial. With these idempotents, we are able to prove that the Mahler measure of the colored Jones polynomial of a sequence of knots obtained by insert linear combination of these idempotents with monomial coefficients converges to the Mahler measure of some 2-variable polynomial, which is a generalized version of the main theorem in [CK]. This chapter is based on a joint work with Patrick Gilmer and Robb Todd in [CGT].

The topological quantum field theory is proposed by Atiyah in [A]. In the revolutionary paper [W], Witten gives the frame work of $2+1$-dimensional topological quantum field theory. Reshetikhin and Turaev [RT] gave a rigorous development of this theory using theory of quantum groups. Then in [BHMV2], a version of $2+1$-dimensional topological quantum field from quantum invariants is rigorously constructed using skein theory. The quantum invariants of 3-manifolds could be recovered from this topological quantum field theory. Moreover, it generates invariants for cobordisms. In [G1, G2, G3], Turaev-Viro endomorphism of a knot is extensively studied using this topological quantum field theory. For each knot, a cobordsim is constructed using 0-surgery on the knot in S^3. Then the strong shift equivalence class of the invariant of this cobordism resulting from the topological quantum field theory is an invariant of the knot.

In Chapter **??**, we construct a $S^2 \times I$ cobordism from S^2 with n points to itself using surgery representation of a knot presented in [R1] and using an idea of Ohtsuki [O1]. Then by applying the TQFT in [BHMV2], we obtain a linear map from this cobordism. We show that the strong shift equivalence class of this map is a knot invariant and it is simpler way to compute the Turaev-Viro endomorphism. This chapter is based on the joint work with Patrick Gilmer [CG].

Chapter 2
Lickorish's Determinant

2.1 Introduction

In [W], Witten proposed the existence of 3-manifold invariants. A mathematically rigorous definition was given by Reshetikhin and Turaev [RT] using quantum groups and Kirby calculus [K]. Later, Lickorish [Li5] provided an alternative proof by using a bilinear form on the Temperley-Lieb algebra TL_n. An important property Lickorish needed was that this bilinear form defined over $\mathbb{Z}[A, A^{-1}]$ is degenerate at certain $4(n+1)$th roots of unity and nondegenerate at $4i$th roots of unity for $i < n+1$. Ko and Smolinsky obtained this result by using a recursive formula for the determinants of specific minors of this form [KS]. They did not give a closed form for the determinant. This was first done by Di Francesco, Golinelli and Guitter [DGG]. Di Francesco later gave a simpler proof. In this paper, we give a short derivation by using a skein-theoretic approach together with a combinatorial proposition from Di Francesco [DiF]. In order to do this, we construct a nice basis $\mathfrak{D}_n$ for TL_n. In fact, there have been several bases of TL_n studied before. See [DGG], [DiF], or [GS]. It turns out that $\mathfrak{D}_n$ is a rescaled version of the basis used in [DiF], but the properties of Jones-Wenzl idempotents significantly simplify the calculation. Our skein-theoretic approach is motivated by the colored graph basis for TQFT modules developed in Blanchet, Habegger, Masbaum, Vogel's paper [BHMV2]. A skein theoretic derivation of a Gram determinant for the type B Temperley-Lieb algebra is given in [CP].

2.2 Temperley-Lieb Algebra

Let F be an oriented surface with a finite collection of points specified in its boundary ∂F. A link diagram in the surface F consists of finitely many arcs and closed curves in F, with a finite number of transverse crossings, each assigned over or under information. The endpoints of the arcs must be the specified points in ∂F. We define the skein of F as follows:

Definition 2.2.1. Suppose A is a variable. Let Λ be the ring $\mathbb{Z}[A, A^{-1}]$ localized by inverting the multiplicative set generated by elements of $\{A^n - 1 \mid n \in \mathbb{Z}^+\}$. The linear skein $\mathcal{S}(F)$ is the module of formal linear sums over Λ of link diagrams in F quotiented by the submodule generated by the skein relations:

1. $L \cup U = \delta L$, where U is a trivial knot, L is a link in F and $\delta = (-A^{-2} - A^2)$;

2.  $=$ A^{-1}  $+$ A  .

Now, taking F to be the 2-disk $D^2 = I \times I$, we have:

Definition 2.2.2. The nth Temperley-Lieb Algebra TL_n is the linear skein $\mathcal{S}(D^2, n)$, where n means there are n points specified in $I \times \{0\}$ and $I \times \{1\}$ respectively.

It is well known that TL_n has a basis, which consists of non-crossing figures. We denote this basis by $\mathfrak{B}_n$. Some special elements $\{1, e_1, ..., e_{n-1}\}$ of the basis are shown in Figure 2.1. As an algebra, TL_n is generated by those elements.

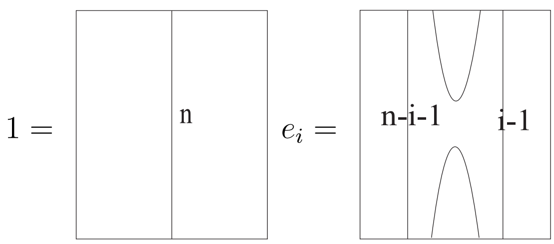

FIGURE 2.1. The integer i beside the arc means i parallel copies of the arc.

A significant property of this algebra used in quantum invariant theory is that there is a natural bilinear form on TL_n. In [Li5], Lickorish used this form to construct quantum invariants of 3-manifolds. We construct this bilinear form with respect to the basis $\mathfrak{B}_n$ that we gave above:

Definition 2.2.3. Define a map on $\mathfrak{B}_n \times \mathfrak{B}_n$ to Λ as follows:

$G_n(s, r) = <$ 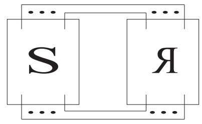 $>$,

where $s =$ 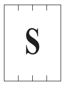 and $r =$  are elements in $\mathfrak{B}_n$ and $<, >$ is the Kauffman bracket. We extend this map to a bilinear form on TL_n, and still denote it by G_n. We denote the determinant of G_n with respect to $\mathfrak{B}_n$ by $\det(G_n)$.

In this paper, we give a simple proof of the determinant of this bilinear form with respect to the basis $\mathfrak{B}_n$, which was also proved in [DGG]. The following is the main result.

Theorem 2.2.4.

$$\det(G_n) = \Delta_1^{c_n} \prod_{k=1}^{n} (\frac{\Delta_k}{\Delta_{k-1}})^{\alpha_k}$$

where

$$\Delta_i = \frac{(-1)^i (A^{2(i+1)} - A^{-2(i+1)})}{A^2 - A^{-2}},$$

$$c_n = \frac{1}{n+1} \begin{pmatrix} 2n \\ n \end{pmatrix}$$

and

$$\alpha_k = \begin{pmatrix} 2n \\ n-k \end{pmatrix} - \begin{pmatrix} 2n \\ n-k-1 \end{pmatrix}.$$

Remark 2.2.5. From now on, we will use Card to denote the cardinality of a set and det the determinant of a matrix.

2.3 Properties of TL_n

In the 1990's, the properties of TL_n were studied by Lickorish [Li6], Masbaum-Vogel [MV], Kauffman-Lins [KL] and some other people. Below we will summarize some results on TL_n that we will be using.

In each Temperley-Libe algebra, there is an idempotent, which is very important in constructing 3-manifold invariants. We will mainly use these idempotent to construct a basis for TL_n. They are defined as follows:

Proposition 2.3.1. *There is a unique element $f_n \in TL_n$, called nth Jones-Wenzl idempotent, such that*

1. $f_n e_i = 0 = e_i f_n$ *for* $1 \leq i \leq n-1$*;*
2. $(f_n - 1)$ *belongs to the subalgebra generated by* $e_1, ..., e_{n-1}$*;*
3. $f_n f_n = f_n$.

Remark 2.3.2. We can put a box on the segment to denote the idempotent. But we will abbreviate the box from now on. Hence, we put an n beside the string to denote n parallel strings with an idempotent inserted, if otherwise is not stated. For example, we denote the figure on the left in Figure 2.2 by the figure on the right, which will be used frequently in this paper.

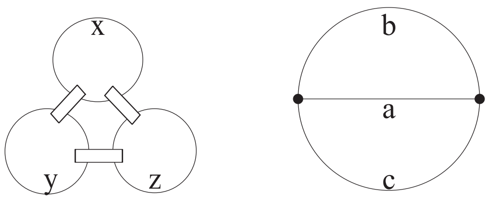

FIGURE 2.2. The left figure lies in S^2. The right figure is an abbreviation of the left one, where $a = x + y, b = y + z, c = x + z$. We denote the value of this diagram in $\mathcal{S}(S^2)$by $\Theta(a, b, c)$.

For the next property, we first set up some notation. Consider the skein space of the disc D with $a+b+c$ specified points on its boundary. The points are partitioned into three sets of a, b, c consecutive points. The effect of adding the idempotents f_a, f_b, f_c just outside every diagram in such a disc with specified points is to map the skein space of the disc into a subspace of itself. We denote this subspace by $T_{a,b,c}$.

Definition 2.3.3. The triple (a, b, c) of nonnegative integers will be called admissible if $a + b + c$ is even, $a \leq b + c$ and $b \leq c + a$ and $c \leq a + b$.

Proposition 2.3.4.

$$dim(T_{a,b,c}) = \begin{cases} 0 & \textit{if } a, b, c \textit{ are not admissible}; \\ 1 & \textit{if } a, b, c \textit{ are admissible.} \end{cases}$$

When (a, b, c) is admissible, $T_{a,b,c}$ has a generator g on the left in Figure 2.3. We usually denote it in a simple way by the diagram on the right in the figure.

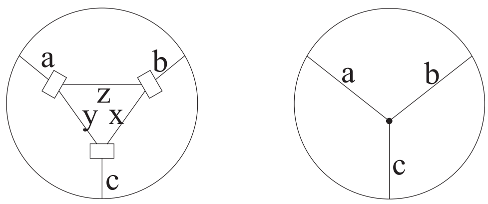

FIGURE 2.3. On the left is the generator of $T_{a,b,c}$. On the right is an abbreviation of the generator.

Proposition 2.3.5.

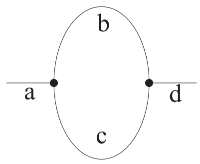

$$= \frac{\delta_{ad}\Theta(a, b, c)}{\Delta_a}$$

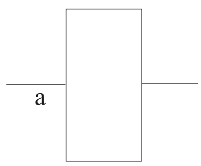

,

where δ_{ad} is the Kronecker delta.

Similarly, consider the skein space of the disc D with $a+b+c+d$ specified points on its boundary. The points are partitioned into four sets of a, b, c, d consecutive points. The effect of adding the idempotents f_a, f_b, f_c, f_d just outside every diagram in such a disc with specified points is to map the skein space of the disc into a subspace of itself. We denote this subspace by $Q_{a,b,c,d}$.

Proposition 2.3.6. *A base for $Q_{a,b,c,d}$ is the set of elements as in Figure 2.4, where j takes all values for which both (a,b,j) and (c,d,j) are admissible.*

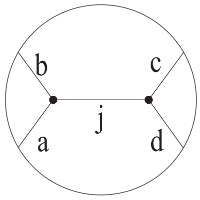

FIGURE 2.4. A basis element of $Q_{a,b,c,d}$

Proposition 2.3.7.

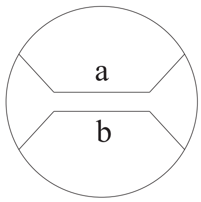

$$= \sum \frac{\Delta_j}{\Theta(a,b,j)}$$

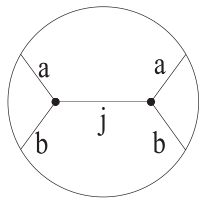

where the summation runs over all j's such that (a,b,j) is admissible.

Remark 2.3.8. We denote $\frac{\Theta(a,b,1)}{\Delta_a}$ by $\Gamma(b,a)$. It is easy to see that $\Gamma(b,a) = 0$ if $\|a-b\| > 1$. Then Proposition 2.3.5 becomes

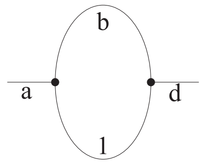

$$= \delta_{ad}\Gamma(b,a)$$

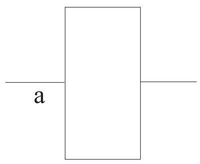

.

2.4 A Basis for the Temperley-Lieb Algebra

Several bases of TL_n have been given before by, for example, [DGG] and [GS]. The idea of constructing the basis in this paper is motivated by [BHMV2] and [Li3]. They constructed bases for modules associated to surfaces by a certain topological quantum field theory. These bases were indexed by coloring of a trivalent graph in a handlebody.

Definition 2.4.1. Let $D_{a_1,\ldots,a_{2n-1}}$ be the element of TL_n in the Figure 2.5 where a_i satisfies:

1. $a_1 = a_{2n-1} = 1$;

2. $a_i \in \mathbb{N}$ for all i;

3. $\|a_i - a_{i-1}\| = 1$ for all i.

Let $\mathfrak{A}_n$ be the collection of all n-tuples $(a_1, ..., a_{2n-1})$ satisfying the above conditions, and let $\mathfrak{D}_n$ be the collection of all these D's.

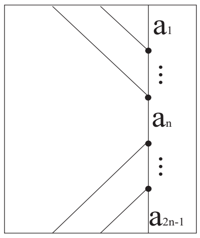

FIGURE 2.5. Each triple point is admissible.

Lemma 2.4.2. *Suppose* $(a_1, ..., a_{2n-1})$ *and* $(b_1, ..., b_{2n-1})$ *satisfy all conditions above except* $a_1 = a_{2n-1} = 1$. *Then*

$$\begin{aligned} &\langle D_{a_1,...,a_{2n-1}}, D_{b_1,...,b_{2n-1}} \rangle \\ = \quad & \Delta_{a_{2n-1}} \prod_{j=1}^{2n-1} \delta_{a_j b_j} \prod_{j=1}^{2n-2} \frac{\theta(a_{j+1}, a_j, i)}{\Delta_{a_{j+1}}} \end{aligned}$$

Proof. We prove the formula by induction.

When $n = 2$, by direct computation,

$$\begin{aligned} &\langle D_{a_1,a_2,a_3}, D_{b_1,b_2,b_3} \rangle \\ = \quad & \delta_{a_1 b_1} \Gamma(a_1, a_2) \delta_{a_2 b_2} \Gamma(a_2, a_3) \delta_{a_3 b_3} \Delta_{a_3}. \end{aligned}$$

Thus the formula is true for $n = 2$. Now suppose the formula is true for $n = k - 1$ and let $n = k$.

$$\begin{aligned}
&\langle D_{a_1,\ldots,a_{2n-1}}, D_{b_1,\ldots,b_{2n-1}} \rangle \\
= \;& \delta_{a_1 b_1} \Gamma(a_1, a_2) \delta_{a_{2n-1} b_{2n-1}} \Gamma(a_{2n-2}, a_{2n-1}) \langle D_{a_2,\ldots,a_{2n-2}}, D_{b_2,\ldots,b_{2n-2}} \rangle \\
= \;& \delta_{a_1 b_1} \Gamma(a_1, a_2) \delta_{a_{2n-1} b_{2n-1}} \Gamma(a_{2n-2}, a_{2n-1}) \times \\
& \delta_{a_2 b_2} \ldots \delta_{a_{2n-2} b_{2n-2}} \Gamma(a_2, a_3) \Gamma(a_3, a_4) \Gamma(a_{2n-3}, a_{2n-2}) \Delta_{a_{2n-2}} \\
= \;& \delta_{a_1 b_1} \ldots \delta_{a_{2n-1} b_{2n-1}} \Gamma(a_1, a_2) \Gamma(a_2, a_3) \ldots \Gamma(a_{2n-2}, a_{2n-1}) \Delta_{a_{2n-1}}.
\end{aligned}$$

Thus the formula holds for $n = k$. Hence, by induction, the formula holds. □

Lemma 2.4.3. *The elements of* $\{D_{a_1,\ldots,a_{2n-1}}\}$ *are orthogonal in* TL_n*, and so are linearly independent.*

Proof. This follows from Lemma 2.4.2. □

Now, we are going to prove that the elements of $\mathfrak{D}_n$ generate TL_n. This can be proved using induction and Proposition 2.3.1 and 2.3.4. For variety, we give an alternative proof.

Lemma 2.4.4. *Each element of* $\{1, e_1, ..., e_{n-1}\}$ *can be expressed as a linear combination of D's in* $\mathfrak{D}_n$.

Proof. We prove the lemma by induction and Proposition 2.3.7. It is easy to see that the lemma is true for $\mathfrak{D}_1, \mathfrak{D}_2$. Suppose the lemma is true for $\mathfrak{D}_{n-1}$, we need show that it is true for $\mathfrak{D}_n$. For $x \in \{1, e_2, e_3, ..., e_{n-1}\}$, we can obtain the result as in Figure 2.6. The proof for e_1 is similar except at the second equality, we use Proposition 2.3.7 for each turn-back, see Figure 2.7. □

Lemma 2.4.5. $\mathfrak{D}_n$ *is a basis of* TL_n.

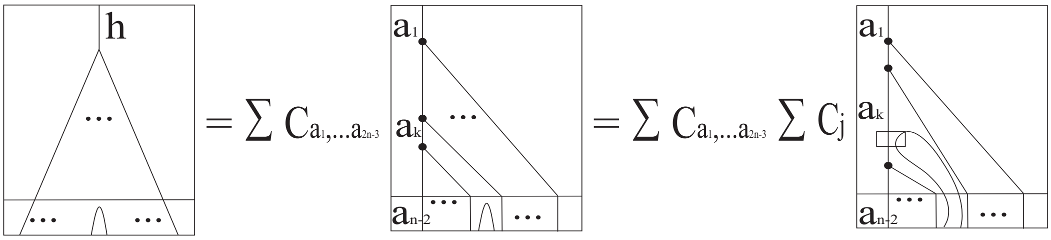

FIGURE 2.6. $x's$ is a generator for TL_{n-1} by deleting the first arc in x. The first equality is from induction step. The second equality is from Proposition 2.3.7.

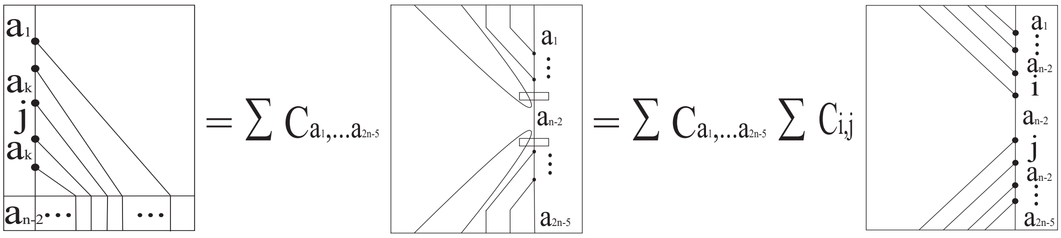

FIGURE 2.7. The proof is the same as in Figure 2.6 except we need use Proposition 2.3.7 twice.

Proof. Since each element in $\mathfrak{B}_n$ can be written as a product of e_i's, we can write each as a sum of products of elements in $\mathfrak{D}_n$ by Lemma 2.4.4. Moreover, a product of elements in $\mathfrak{D}_n$ can be written as a linear combination of elements in $\mathfrak{D}_n$ by Proposition 2.3.5. So we can write elements in $\mathfrak{B}_n$ as sums of elements in $\mathfrak{D}_n$. As $\mathfrak{B}_n$ is a basis for TL_n, the lemma holds. □

2.5 Relation between $\mathfrak{B}_n$ and $\mathfrak{D}_n$

In this section, we will give a new system to denote the basis $\mathfrak{B}_n$. We draw a diagram similar to elements in $\mathfrak{D}_n$ as in Figure 2.8, except we do not put idempotents on strings and we put an empty circle at each black triple point. If $a_i = a_{i+1} + 1$, we put Figure 2.9 in the corresponding circle. If $a_i = a_{i+1} - 1$, then we put Figure 2.10 in the corresponding circle. After filling all circles, we get a non-crossing diagram in TL_n for each sequence $(a_1, ..., a_{2n-1})$, which satisfies the conditions in Definition 2.4.1. Those elements belong to $\mathfrak{B}_n$. Now, we give a total order on the set $\mathfrak{A}_n$ as follows: $(a_1, ..., a_{2n-1}) < (b_1, ..., b_{2n-1})$ if there is a j such that $a_i = b_i$ for all $i < j$ and $a_j < b_j$. This order on $\mathfrak{A}_n$ induces an order on $\{B_{a_1,...,a_{2n-1}}\}$ and $\mathfrak{D}_n$

naturally. In this order, we will show that the representing matrix of $\{B_{a_1,\ldots,a_{2n-1}}\}$ with respect to basis $\mathfrak{D}_n$ is upper triangular having 1's on the diagonal.

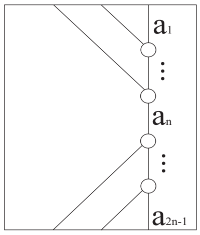

FIGURE 2.8. An example of $B_{a_1,\ldots,a_{2n-1}}$.

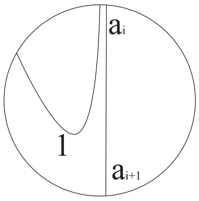

FIGURE 2.9. $a_i = a_{i+1} + 1$

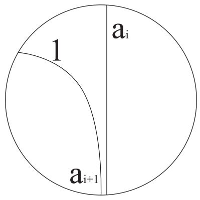

FIGURE 2.10. $a_i = a_{i+1} - 1$

Lemma 2.5.1. $\langle B_{a_1,a_2,\ldots,a_{2n-1}}, D_{b_1,b_2,\ldots,b_{2n-1}}\rangle = 0$ *if* $(a_1, a_2, \ldots, a_{2n-1}) < (b_1, b_2, \ldots, b_{2n-1})$.

Proof. Since $(a_1, a_2, \ldots, a_{2n-1}) < (b_1, b_2, \ldots, b_{2n-1})$, there is a j such that $a_j < b_j$. If we pair $B_{a_1,a_2,\ldots,a_{2n-1}}$ and $D_{b_1,b_2,\ldots,b_{2n-1}}$ together, we can find a circle passing through them at a_j and b_j. We cut the pairing along this circle to get an element as in Figure 2.11. By the properties of idempotents, it is easy to see that this element is 0 in $\mathcal{S}(D^2)$ with a_j and b_j on the boundary. So we get the result. □

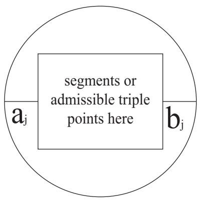

FIGURE 2.11. We have the idempotent at b_j and no idempotent at a_j.

Before we go on, we introduce a lemma and a corollary.

Lemma 2.5.2. $\Theta(n, n+1, 1) = \Delta_{n+1}$, *and* $\Theta(n, n-1, 1) = \Delta_n$.

Proof.

$$\Theta(n, n+1, 1)$$

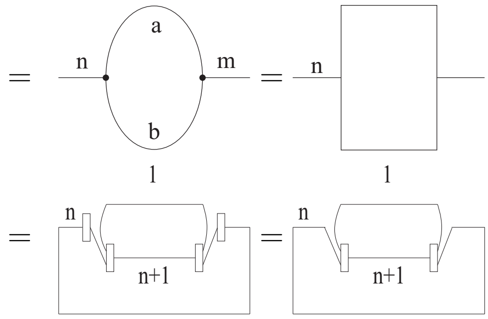

$$= \quad \Delta_{n+1}$$

Similarly, it is easy to see that $\Theta(n, n-1, 1) = \Delta_n$. $\square$

Corollary 2.5.3.

$$\Gamma(b, a) = \begin{cases} 1 & \textit{if } a = b+1, \\ \frac{\Delta_{a+1}}{\Delta_a} & \textit{if } a = b-1. \end{cases}$$

Proof. This follows easily from Lemma 2.5.2. $\square$

Now, we can prove the following:

Proposition 2.5.4. $\langle B_{a_1,a_2,...,a_{2n-1}}, D_{a_1,a_2,...,a_{2n-1}} \rangle = \langle D_{a_1,a_2,...,a_{2n-1}}, D_{a_1,a_2,...,a_{2n-1}} \rangle$ *for all* $(a_1, a_2, ..., a_{2n-1})$ *in* $\mathfrak{A}_n$.

Proof. We prove this by induction on n. Suppose $n = 2$. Then it is easy to check that

$$\langle B_{1,0,1}, D_{1,0,1} \rangle = \langle D_{1,0,1}, D_{1,0,1} \rangle, \langle B_{1,2,1}, D_{1,2,1} \rangle = \langle D_{1,2,1}, D_{1,2,1} \rangle.$$

Assume that the result is true for $n < k$. We will prove it is true for $n = k$. For $(a_1, ..., a_{2n-1}) = (1, 2, ..., k, ..., 2, 1)$, we have

$$\langle B_{1,2,...,k,...,2,1}, D_{1,2,...,k,...,2,1} \rangle = \langle D_{1,2,...,k,...,2,1}, D_{1,2,...,k,...,2,1} \rangle$$

by direct computation. For $(a_1, ..., a_{2n-1}) \neq (1, 2, ..., k, ..., 2, 1)$, we choose $i > k > j$ such that $a_{i-1} = a_{i+1}$, $a_{j-1} = a_{j+1}$ and $a_i = a_{i-1} + 1$, $a_j = a_{j-1} + 1$. Then by Proposition 2.3.5, we have

$$\begin{aligned} & \langle B_{a_1,a_2,...,a_{2n-1}}, D_{a_1,a_2,...,a_{2n-1}} \rangle \\ = \; & \Gamma(a_i, a_{i+1})\Gamma(a_j, a_{j+1}) \\ & \times \langle B_{a_1,...,\hat{a}_i,\hat{a}_{i+1},...\hat{a}_j,\hat{a}_{j+1},...,a_{2n-1}}, D_{a_1,...,\hat{a}_i,\hat{a}_{i+1},...,\hat{a}_j,\hat{a}_{j+1},...,a_{2n-1}} \rangle \end{aligned}$$

where the hat on a_i means that it is removed.

It is easy to see that

$$B_{a_1,...,\hat{a}_i,\hat{a}_{i+1},...\hat{a}_j,\hat{a}_{j+1},...,a_{2n-1}} \in \mathfrak{B}_{n-2}, D_{a_1,...,\hat{a}_i,\hat{a}_{i+1},...,\hat{a}_j,\hat{a}_{j+1},...,a_{2n-1}} \in \mathfrak{D}_{n-2}.$$

By Lemma 2.4.2 and Corollary 2.5.3,

$$\begin{aligned} & \langle D_{a_1,a_2,...,a_{2n-1}}, D_{a_1,a_2,...,a_{2n-1}} \rangle \\ = \; & \Gamma(a_i, a_{i+1})\Gamma(a_j, a_{j+1}) \\ & \times \langle D_{a_1,...,\hat{a}_i,\hat{a}_{i+1},...\hat{a}_j,\hat{a}_{j+1},...,a_{2n-1}}, D_{a_1,...,\hat{a}_i,\hat{a}_{i+1},...,\hat{a}_j,\hat{a}_{j+1},...,a_{2n-1}} \rangle. \end{aligned}$$

By induction,

$$\begin{aligned} & \langle B_{a_1,...,\hat{a}_i,\hat{a}_{i+1},...\hat{a}_j,\hat{a}_{j+1},...,a_{2n-1}}, D_{a_1,...,\hat{a}_i,\hat{a}_{i+1},...,\hat{a}_j,\hat{a}_{j+1},...,a_{2n-1}} \rangle \\ = \; & \langle D_{a_1,...,\hat{a}_i,\hat{a}_{i+1},...\hat{a}_j,\hat{a}_{j+1},...,a_{2n-1}}, D_{a_1,...,\hat{a}_i,\hat{a}_{i+1},...,\hat{a}_j,\hat{a}_{j+1},...,a_{2n-1}} \rangle. \end{aligned}$$

Hence,

$$\langle B_{a_1,a_2,...,a_{2n-1}}, D_{a_1,a_2,...,a_{2n-1}} \rangle = \langle D_{a_1,a_2,...,a_{2n-1}}, D_{a_1,a_2,...,a_{2n-1}} \rangle.$$

□

Proposition 2.5.5.

$$\begin{pmatrix} B_{1,2,\ldots,n,\ldots,1} \\ \vdots \\ B_{1,0,1,0,\ldots,0,1} \end{pmatrix} = \begin{pmatrix} 1 & * & \cdots & * \\ 0 & 1 & \cdots & * \\ \vdots & \vdots & \ddots & \vdots \\ 0 & 0 & \cdots & 1 \end{pmatrix} \begin{pmatrix} D_{1,2,\ldots,n,\ldots,1} \\ \vdots \\ D_{1,0,1,0,\ldots,0,1} \end{pmatrix}.$$

Proof. This follows easily from Lemma 2.5.1 and Proposition 2.5.4. □

Corollary 2.5.6. $\{B_{a_1,\ldots,a_{2n-1}}\} = \mathfrak{B}_n$.

Proof. By Proposition 2.5.5, we can see that $B_{a_1,\ldots,a_{2n-1}} \neq B_{b_1,\ldots,b_{2n-1}}$ if $(a_1, \ldots, a_{2n-1}) \neq (b_1, \ldots, b_{2n-1})$. Moreover, $\mathrm{Card}\{B_{a_1,\ldots,a_{2n-1}}\} = \mathrm{Card}\,\mathfrak{D}_n = \mathrm{Card}\,\mathfrak{B}_n$ and $\{B_{a_1,\ldots,a_{2n-1}}\} \subset \mathfrak{B}_n$. So we have $\{B_{a_1,\ldots,a_{2n-1}}\} = \mathfrak{B}_n$. □

By Corollary 2.5.6 and linear algebra, we can see that the $\det(G_n)$ we get by using the basis $\mathfrak{B}_n$ is the same as $\det(G_n)$ we get by using the basis $\mathfrak{D}_n$.

2.6 Lattice Path

Definition 2.6.1. A lattice path in the plane is a path from $(0,0)$ to (a,b) with northeast and southeast unit steps, where $a, b \in \mathbb{Z}$. A Dyck path is a lattice path that never goes below the $x-$axis. We denote the set of all Dyck path from $(0,0)$ to (a,b) by $\mathcal{D}_{(a,b)}$.

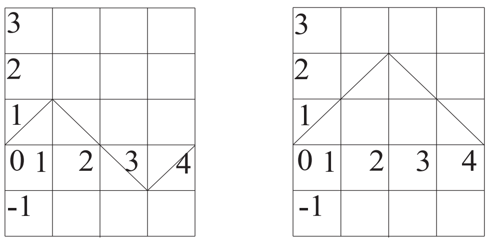

FIGURE 2.12. On the left is a lattice path. On the right is a Dyck path.

Remark 2.6.2. There is a natural bijection f from $\mathfrak{D}_n$ to $\mathcal{D}_{(2n,0)}$, the set of all Dyck paths from $(0,0)$ to $(2n,0)$ as follows:

For each $D_{a_1,\ldots,a_{2n-1}} \in \mathfrak{D}_n$, we construct a path from $(0,0)$ to $(2n,0)$ with step (i,a_i) for all $1 \leq i \leq 2n-1$. Since a_i satisfies

1. $a_1 = a_{2n-1} = 1$;

2. $a_i \in \mathbb{N}$ for all i;

3. $\|a_i - a_{i-1}\| = 1$ for all i.

We can see that this is a Dyck path.

Remark 2.6.3. The reflection principle [C, page 22] says that the number of all Dyck paths from $(0,0)$ to $(2n,0)$ is the Catalan number $C_n = \frac{1}{n+1}\binom{2n}{n}$. Hence, we recover the well-known result that the dimension of TL_n is C_n.

2.7 Proof of the Main Theorem

Now we can start our proof of the main theorem. By Lemma 2.4.3, we know that $\{D_{a_1,\ldots,a_{2n-1}}\}$ is an orthogonal basis with respect to the bilinear form. Thus the matrix of G_n is a diagonal matrix under this basis. We have

$$\det(G_n) = \prod_{(a_1,\ldots,a_{2n-1})} \langle D_{a_1,\ldots,a_{2n-1}}, D_{a_1,\ldots,a_{2n-1}} \rangle.$$

Then by Lemma 2.4.2, we have

$$\det(G_n) = \prod_{(a_1,\ldots,a_{2n-1})} \Gamma(a_1,a_2)\Gamma(a_2,a_3)\ldots\Gamma(a_{2n-2},a_{2n-1})\Delta_1.$$

Using Lemma 2.5.3, we can simplify $\det(G_n)$ as follows:

Consider the tuple (D,i) such that D is an element of $\mathfrak{D}_n$ and $a_i = k$ in D. If $a_{i+1} = k+1$, then $\Gamma(a_i,a_{i+1})$ is 1 by Lemma 2.5.3. So (D,i) will contribute 1 to $\det(G_n)$. If $a_{i+1} = k-1$, then $\Gamma(a_i,a_{i+1}) = \frac{\Delta_{k+1}}{\Delta_k}$. So (D,i) will contribute $\frac{\Delta_k}{\Delta_{k-1}}$ to $\det(G_n)$. We denote by $\mathfrak{S}_k$ the set of all tuple $\{(D,i)\}$ with $D \in \mathfrak{D}_n$ and

$a_i = k, a_{i+1} = k-1$ in D. Let α_k be the cardinality of $\mathfrak{S}_k$. Then

$$\det(G_n) = \Delta_1^{\operatorname{Card}\mathfrak{D}_n} \prod_{k=1}^{n} (\frac{\Delta_k}{\Delta_{k-1}})^{\alpha_k} .$$

Now, the theorem is reduced to calculate α_k for each k.

Proposition 2.7.1.

$$\alpha_k = \begin{pmatrix} 2n \\ n-k \end{pmatrix} - \begin{pmatrix} 2n \\ n-k-1 \end{pmatrix}.$$

Proof. In Section 2.6, we already had a 1-1 correspondence f between $\mathfrak{D}_n$ (the new basis we constructed) and $\mathcal{D}_{(2n,0)}$ (Dyck paths from $(0,0)$ to $(2n,0)$). With respect to this correspondence, each pair (D,i) in $\mathfrak{S}_k$ is associated to a pair $(f(D),i)$ with $a_i = k, a_{i+1} = k-1$ in $f(D)$, that is the step from $(i, a_i = k)$ to $(i+1, a_{i+1} = k-1)$ in the path $f(D)$. See Figure 2.13 for an example. Denote by $\mathcal{S}_k$ the set of all pairs $(f(D),i)$, where $f(D)$ has a step from k to $k-1$ at i. Thus we have a 1-1 correspondence between $\mathfrak{S}_k$ and $\mathcal{S}_k$. Di Francesco [DiF, page 562] set up a 1-1

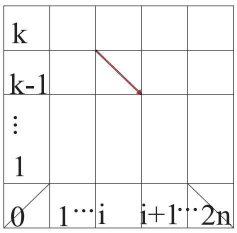

FIGURE 2.13. The bold step is a step going down from $(i, a_i = k)$ to $(i+1, a_{i+1} = k-1)$.

correspondence from $\mathcal{S}_k$ to $\mathcal{D}_{(2n,2k)}$. Then we have

$$\alpha_k = \operatorname{Card}\mathcal{D}_{(2n,2k)} = \begin{pmatrix} 2n \\ n-k \end{pmatrix} - \begin{pmatrix} 2n \\ n-k-1 \end{pmatrix}.$$

For the convenience of reader, we now give Di Francesco's correspondence in our terminology. For an element $\hat{P} \in \mathcal{D}_{(2n,2k)}$, it should intersect the horizontal line $y = k$ in a point $p = (i, a_i = k)$ with $a_{i+1} = k+1$ and $a_{i-1} = k-1$ at least once.

Let p be the rightmost such intersection. Now we cut $\hat{P}$ at the point p, reflect the right part of $\hat{P}$ with respect to y-axis, and shift it down by k units. Then we glue this part back to the left part. We get a Dyck path P from $(0,0)$ to $(2n,0)$. In the resulting path P, we then choose the smallest $i' \geq i$, such that $a_i' = k$ and $a_{i'+1} = k-1$. We associate the path $\hat{P}$ to the pair (P,i'). Therefore, we construct a map $\phi : \mathcal{D}_{(2n,2k)} \to \mathcal{S}_k$.

Conversely, for a pair (P,i), where $P \in \mathcal{D}_{(2n,0)}$. We choose the largest $i' \leq i$ with $a_{i'} = k$ and $a_{i'-1} = k-1$. We cut the path P at i', reflect the right part with respect to the y-axis, shift up by n units and glue it back. Thus we construct a path $\hat{P}$ in $\mathcal{D}_{(2n,2k)}$. We associate the tuple (P,i) to the path $\hat{P}$. Therefore, we construct a map $\varphi : \mathcal{S}_k \to \mathcal{D}_{(2n,2k)}$.

It is easy to see that $\phi\varphi = id$ and $\varphi\phi = id$. Therefore, we have constructed a 1-1 correspondence between $\mathcal{S}_k$ and $\mathcal{D}_{(2n,2k)}$.

By the reflection principle, we have

$$\operatorname{Card} \mathcal{D}_{(2n,2k)} = \begin{pmatrix} 2n \\ n-k \end{pmatrix} - \begin{pmatrix} 2n \\ n-k-1 \end{pmatrix}.$$

Therefore, we have

$$\alpha_k = \begin{pmatrix} 2n \\ n-k \end{pmatrix} - \begin{pmatrix} 2n \\ n-k-1 \end{pmatrix}.$$

$\square$

2.8 Relation between $\mathfrak{D}_n$ and Di Francesco's second basis.

In this section, we extend our ring Λ to the complex numbers $\mathbb{C}$ and let A be any non-zero complex number which is not a root of unity.

Definition 2.8.1.

$$ND_{a_1,\dots,a_{2n-1}} = \frac{D_{a_1,\dots,a_{2n-1}}}{< D_{a_1,\dots,a_{2n-1}}, D_{a_1,\dots,a_{2n-1}} >^{\frac{1}{2}}}.$$

We call $ND_{a_1,\dots,a_{2n-1}}$ the normalization of $D_{a_1,\dots,a_{2n-1}}$, and denote the normalized basis by $\mathfrak{N}\mathfrak{D}_n$.

Theorem 2.8.2. *$\mathfrak{N}\mathfrak{D}_n$ is the same basis as Di Francesco's second basis in [DiF].*

Proof. Di Francesco defined his orthonormal basis by a recursive equation [DiF, equation 3.19, Page 555]. So we just need to show that $\mathfrak{N}\mathfrak{D}_n$ satisfies the recursive equation and the initial condition.

Let $D_{a_1,\dots,a_{i-1},a_i,a_{i+1},\dots,a_{2n-1}}$ and $D_{a_1,\dots,a_{i-1},a'_i,a_{i+1},\dots,a_{2n-1}}$ be two elements in $\mathfrak{D}_n$ such that $a_i = a_{i-1} - 1 = a_{i+1} - 1$ and $a'_i = a_i + 2$, that means they are equal everywhere except at ith arc. Then using the recursive formula for Jones-Wenzl idempotents at ith arc, we have

$$D_{a_1,\dots,a_{i-1},a_{i'},a_{i+1},\dots,a_{2n-1}} = D_{a_1,\dots,a_{i-1},\hat{a}_i,a_{i+1},\dots,a_{2n-1}} - \frac{\Delta_{a_i}}{\Delta_{a_i+1}} D_{a_1,\dots,a_{i-1},a_i,a_{i+1},\dots,a_{2n-1}}$$

where $D_{a_1,\dots,a_{i-1},\hat{a}_i,a_{i+1},\dots,a_{2n-1}}$ is as in Figure 2.14. Since $a_{i-1} = a_{i+1}$, this is well

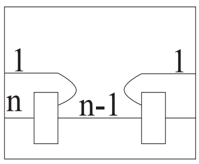

FIGURE 2.14. a_i disappears.

defined. It is easy to see that $D_{a_1,\dots,a_{i-1},\hat{a}_i,a_{i+1},\dots,a_{2n-1}} = e_i D_{a_1,\dots,a_{i-1},a_i,a_{i+1},\dots,a_{2n-1}}$, where e_i acts on $D_{a_1,\dots,a_{i-1},a_i,a_{i+1},\dots,a_{2n-1}}$ as in [DiF]. We divide the equation by the norm of $D_{a_1,\ldots,a_{i-1},a_{i'},a_{i+1},\ldots,a_{2n-1}}$ on both sides. By Lemma 2.4.2, we have

$$\begin{aligned}
& ND_{a_1,\ldots,a_{i-1},a_i',a_{i+1},\ldots,a_{2n-1}} \\
= \; & \frac{(e_i D_{a_1,\ldots,a_{i-1},a_i,a_{i+1},\ldots,a_{2n-1}} - \frac{\Delta_{a_i}}{\Delta_{a_i+1}} D_{a_1,\ldots,a_{i-1},a_i,a_{i+1},\ldots,a_{2n-1}})}{(\Gamma(a_1,a_2)\ldots\Gamma(a_{i-1},a_i')\Gamma(a_i',a_{i+1})\ldots\Gamma(a_{2n-2},a_{2n-1})\Delta_{a_{2n-1}})^{\frac{1}{2}}} \\
= \; & (e_i - \frac{\Delta_{a_i}}{\Delta_{a_i+1}}) ND_{a_1,\ldots,a_{i-1},a_i,a_{i+1},\ldots,a_{2n-1}} \times \\
& \frac{(\Gamma(a_1,a_2)\ldots\Gamma(a_{i-1},a_i)\Gamma(a_i,a_{i+1})\ldots\Gamma(a_{2n-2},a_{2n-1})\Delta_{a_{2n-1}})^{\frac{1}{2}}}{(\Gamma(a_1,a_2)\ldots\Gamma(a_{i-1},a_i')\Gamma(a_i',a_{i+1})\ldots\Gamma(a_{2n-2},a_{2n-1})\Delta_{a_{2n-1}})^{\frac{1}{2}}} \\
= \; & (e_i - \frac{\Delta_{a_i}}{\Delta_{a_i+1}}) ND_{a_1,\ldots,a_{i-1},a_i,a_{i+1},\ldots,a_{2n-1}} \frac{(\Gamma(a_{i-1},a_i)\Gamma(a_i,a_{i+1}))^{\frac{1}{2}}}{(\Gamma(a_{i-1},a_i')\Gamma(a_i',a_{i+1}))^{\frac{1}{2}}} \\
= \; & (e_i - \frac{\Delta_{a_i}}{\Delta_{a_i+1}}) ND_{a_1,\ldots,a_{i-1},a_i,a_{i+1},\ldots,a_{2n-1}} \frac{(\Gamma(a_{i-1},a_i))^{\frac{1}{2}}}{(\Gamma(a_i',a_{i+1}))^{\frac{1}{2}}} .
\end{aligned}$$

By definition,

$$\Gamma(a_{i-1},a_i) = \mu_{a_i}, \Gamma(a_i',a_{i+1}) = \mu_{a_{i+1}},$$

where μ_i as in [DiF]. Thus, $\mathfrak{N}\mathfrak{D}_n$ satisfies the recursive equation. Moreover, it is easy to see that

$$u_n = ND_{1,0,1,0,\ldots,0,1,0,1},$$

where u_n is as in [DiF, equation 3.5,Page 551]. So $\mathfrak{N}\mathfrak{D}_n$ satisfies the initial condition. $\square$

Chapter 3
Semi-Meander Determinant

3.1 Introduction

Vaughan Jones discovered his famous knot polynomial [J], which triggered the developments relating knot theory, topological quantum field theory, and statistical physics [Ka2] [W] [TL]. A central role in those developments was played by the Temperley-Lieb algebra. Lickorish [Li5] constructed quantum invariants for 3-manifolds from the Temperley-Lieb algebra TL_n. He used a natural bilinear form on TL_n. Our aim is to generalize this skein module and the bilinear form. As a module, the Temperley-Lieb algebra TL_n can be considered as a skein module of a square with $2n$ points on the boundary. Then skein modules of a square with points on the boundary colored by non-negative integers are a natural generalization of TL_n. The same methods [Cai] that the author has employed in studying TL_n may be adapted to this more general situation. In order to understand this, we consider the skein module of a square $S(I \times I, n, h)$ with n points on $I \times \{0\}$ and one point colored h on $I \times \{1\}$. We consider the natural generalization of Lickorish's bilinear form on $S(I \times I, n, h)$, and define the determinant of the bilinear form with respect to a natural basis $\mathcal{B}_n^h$. We find that the determinant that we calculated is related to a semi-meander determinant that was suggested to the author by his advisor Patrick Gilmer. Meander determinants and semi-meander determinants were studied by Di Francesco, Golinelli and Guitter [DGG]. The semi-meander determinant that we study is a generalization of their meander determinant but is different from their semi-meander determinant.

We compute the determinant of the bilinear form using an orthogonal basis $\mathcal{D}_n^h$, which is motivated by [BHMV2]. The transform matrix between $\mathcal{B}_n^h$ and $\mathcal{D}_n^h$ is an upper triangular matrix with 1's on the diagonal. So the determinant we get by using the basis $\mathcal{D}_n^h$ is the same as the determinant we get by using the basis $\mathcal{B}_n^h$. In the calculation, we set up a correspondence between the elements of $\mathcal{D}_n^h$ and generalized Dyck paths on $\mathbb{R}^2$. The problem is then reduced to count certain steps in all generalized Dyck paths from $(0,0)$ to (n,h). In Section 3.5, we present two different proofs for the counting problem. The first method is geometric. It is a generalization of the method used by Di Francesco for the case $h=0$. The second method uses generating functions.

3.2 The Skein Module $S(I \times I, n, h)$

In Chapter 2, we introduce the nth Temperley-Lieb algebra, i.e. the skein module $S(I \times I, n)$. In this chapter, we give one generalization of Temperley-Lieb algebra, which is related to meander determinant. We define this skein module by following Lickorish's idea [Li6, Page 151].

Definition 3.2.1. Suppose we have $a_1 + \ldots + a_n$ points on ∂F. We partition them into n sets of $a_1, \ldots, a_n$ consecutive points and put corresponding Jones-Wenzl idempotent just outside each diagram for each grouped points. All this kind of elements form a subspace of $\mathcal{S}(F, a_1 + \ldots + a_n)$. We call this subspace colored skein module $\mathcal{S}(F; a_1, \ldots, a_n)$ of F with n points on ∂F colored by $a_1, \ldots, a_n$.

Since f_1 is the identity of TL_1, we can consider the normal skein module as the colored skein module of $\mathcal{S}(F, n)$ with coloring $1, \ldots, 1$, i.e.

$$\mathcal{S}(F, n) = \mathcal{S}(F; 1, \ldots, 1).$$

Therefore, colored skein modules generalize the definition of normal skein modules.

Definition 3.2.2. The skein module $\mathcal{S}(I \times I, n, h)$ is the colored skein module of $I \times I$ with $n+1$ points on boundary , n points colored by 1 and 1 point colored by h.

Notation 3.2.3. We put the point colored by h on $I \times \{1\}$ and the n points colored by 1 on $I \times \{0\}$.

Proposition 3.2.4. *There is a natural generating set $\mathcal{B}_n^h$ for $\mathcal{S}(I \times I, n, h)$ consisting of crossing free diagrams with no arc connecting two of the h points in $I \times \{1\}$.*

Proof. For a crossing in a diagram, we just use the second skein relation to smooth it. Then we can smooth all crossings in every diagram. That means every diagram can be written as a linear sum of crossing free diagrams. Therefore, we can get a generating set consisting of crossing free diagrams. Moreover, by Proposition 2.3.1 in Chapter 2, a crossing free diagram with a segment connecting two of the set of h points is 0 in $\mathcal{S}(I \times I, n, h)$. Thus, the result follows. □

Remark 3.2.5. We will see later that actually $\mathcal{B}_n^h$ is a basis of $\mathcal{S}(I \times I, n, h)$. So we will call $\mathcal{B}_n^h$ the natural basis.

We can also generalize the natural bilinear form on TL_n to a bilinear form on $\mathcal{S}(I \times I, n, h)$ as follows:

Proposition 3.2.6. *Suppose A and B are two elements in $\mathcal{S}(I \times I, n, h)$. We define a function:*

$$G : \mathcal{S}(I \times I, n, h) \times \mathcal{S}(I \times I, n, h) \to \Lambda$$

by gluing $I \times \{0\}$ of A to $I \times \{0\}$ of B and $I \times \{1\}$ of A to $I \times \{1\}$ of B and evaluate the resulting diagram by Kauffman bracket. This is a bilinear form on $\mathcal{S}(I \times I, n, h)$.

Proof. This is a standard skein theoretic argument. $\square$

Suppose the matrix of the bilinear form G with respect to the natural basis $\mathcal{B}_n^h$ is B. We will calculate the determinant of B.

Theorem 3.2.7. *We have*

$$\det(B) = \Delta_h^{|\mathcal{D}_n^h|} \prod_k \left(\frac{\Delta_k}{\Delta_{k-1}}\right)^{\alpha_{(n,h)}^k},$$

where $\alpha_{(n,h)}^k = \binom{n}{\frac{n+h+2k-2s}{2}} - \binom{n}{\frac{n+h+2k+2}{2}}$ *for* $s = \min\{k-1, h\}$.

3.3 A New Basis $\mathcal{D}_n^h$

We do not directly compute the determinant of B. In fact, we construct a new basis $\mathcal{D}_n^h$ of $\mathcal{S}(I \times I, n, h)$, which is orthogonal with respect to the bilinear form. We then find the transform matrix between them.

Before we continue, let us set up some notations.

Definition 3.3.1. Three non-negative integers a, b, c are called admissible if they satisfy

1. a+b+c is even;
2. $|b-c| \leq a \leq b+c$.

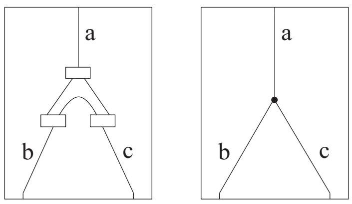

FIGURE 3.1. We denote the figure on the left by the figure on the right

Proposition 3.3.2. *The colored skein module* $\mathcal{S}(D^2; a, b, c)$ *is 1 dimensional if* a, b, c *are admissible,* 0 *dimensional otherwise.*

Proof. This is a standard result in skein theory, see, for example, [Li6] or [KL]. $\square$

Remark 3.3.3. The generator for $\mathcal{S}(D^2; a, b, c)$ is the diagram on the left of Figure 3.1, and we use a trivalent graph with a black dot as the diagram on the right to denote the generator.

Definition 3.3.4. We define an element $D_{a_1,\dots,a_n}$ of $\mathcal{S}(I \times I, n, h)$ as in Figure 3.2, where the black dot is as in Remark 3.3.3, and $a_1, \dots, a_n$ are non-negative integers satisfying the admissible condition at each black dot. Let $\mathcal{D}_n^h$ be the set of such elements.

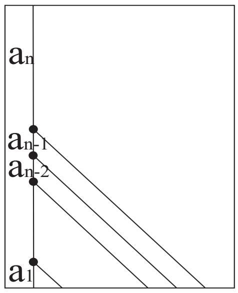

FIGURE 3.2. The new basis element

Remark 3.3.5. It is easy to see that the restrictions on $a_1, \dots, a_n$ are equivalent to the following conditions:

- $a_n = h, a_1 = 1$ and $a_i \geq 0$ for $1 < i < n$;
- $|a_i - a_{i+1}| = 1$ for all $0 < i < n - 1$.

Proposition 3.3.6. *We have*

$$G(D_{a_1,\dots,a_n}, D_{b_1,\dots,b_n}) = \begin{cases} \prod_{i=1}^{n} \frac{\theta(a_{i+1}, a_i, 1)}{\Delta_{a_{i+1}}} & \textit{if } (a_1, \dots, a_n) = (b_1, \dots, b_n); \\ 0 & \textit{else.} \end{cases}$$

Proof. We just need to repeatedly use the following standard result in Figure 3.3 □

Corollary 3.3.7. *The elements $D_{a_1,\dots,a_n}$ are orthogonal with respect to the natural bilinear form.*

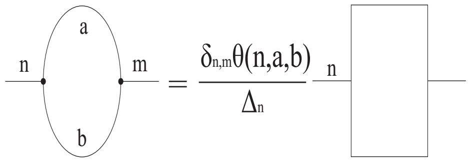

FIGURE 3.3. Here $\delta_{n,m}$ is the Kronecker delta.

Proof. The proof follows immediately from Proposition 3.3.6. □

Proposition 3.3.8. *Each element in $\mathcal{S}(I \times I, n, h)$ can be written as a linear combination of elements in $\mathcal{D}_n^h$.*

Proof. It is sufficient to show the result holds for all elements in $\mathcal{B}_n^h$. We proceed the proof by induction on $n \geq h$. Clearly, the result is true for $\mathcal{B}_h^h$. Suppose the result is true for $\mathcal{B}_k^h$ with $h \leq k \leq n-1$. The proof for the element $\mathcal{B}_n^h$ is obtained easily from Figure 4.4. □

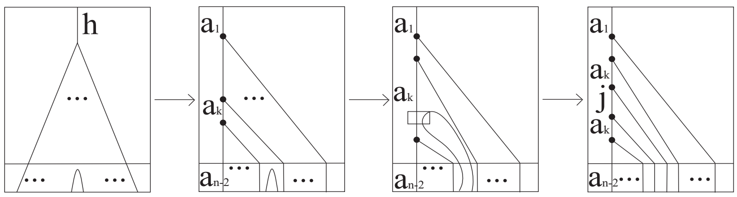

FIGURE 3.4. For an element $x \in \mathcal{B}_n^h$, we consider it as being the composition of two layers as in the first Diagram. The upper half diagram is in $\mathcal{B}_{n-2}^h$. By induction, we can then write x as a linear combination of figures in the second diagram. Next, we pull over the turn-back and apply the Fusion Lemma [KL] in skein theory to the boxed area. We can write x as a linear combination of the figures in the last diagram

Corollary 3.3.9. *The set $\mathcal{D}_n^h$ is a basis for $\mathcal{S}(I \times I, n, h)$.*

Proof. The proof follows immediately from Corollary 3.3.7 and Proposition 3.3.8. □

By the Proposition 3.3.6 and Corollary 3.3.9, we obtain the fact that the matrix of the bilinear form with respect to the basis $\mathcal{D}_n^h$ is diagonal. To calculate its determinant, we just multiply the diagonal entries together. However, we want to calculate the determinant of the bilinear form with respect to the natural basis $\mathcal{B}_n^h$. Thus, we need to find the transformation matrix A between $\mathcal{D}_n^h$ and $\mathcal{B}_n^h$. To do so, we have to align all the elements in $\mathcal{D}_n^h$ and $\mathcal{B}_n^h$. At first, we define a total order on $\mathcal{D}_n^h$ and $\mathcal{B}_n^h$.

Definition 3.3.10. For a set of n-tuples $\{(a_1, \ldots, a_n)\}$, we give a lexigraphic order on it as follows:

- $(a_1, \ldots, a_n) > (b_1, \ldots, b_n)$ if there is a j such that $a_i = b_i$ for all $i < j$ and $a_j > b_j$;
- $(a_1, \ldots, a_n) = (b_1, \ldots, b_n)$ if $a_i = b_i$ for all i;
- $(a_1, \ldots, a_n) < (b_1, \ldots, b_n)$, otherwise.

Since each element in $\mathcal{D}_n^h$ corresponds to an n-tuple, we can give the $\mathcal{D}_n^h$ above total order. We can then align the elements in $\mathcal{D}_n^h$ from the maximum to the minimum vertically. We will assign a new system to denote elements in $\mathcal{B}_n^h$ such that we can do the same thing.

Definition 3.3.11. We construct a new element $B_{a_1,\ldots,a_n}$ of $\mathcal{S}(I \times I, n, h)$ from $D_{a_1,\ldots,a_n}$ as follows. We do not insert corresponding idempotents into segments except for a_n. We delete each black dot in the diagram and put a circle around it. If $a_i = a_{i+1} + 1$, then we put the diagram on the left of Figure 3.5 in the circle. If $a_i = a_{i+1} - 1$, then we put the diagram on the right of Figure 3.5 in the circle.

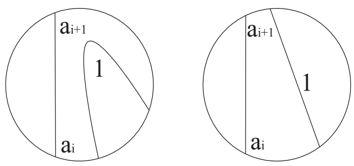

FIGURE 3.5. We fill the circle with those two diagrams according to a_i and a_{i+1}

The proofs of the following two lemmas are very similar to the proofs [C, Lemma 5.1, Proposition 5.4].

Lemma 3.3.12. *For all* n*,*

$$G(D_{a_1,\dots,a_n}, B_{a_1,\dots,a_n}) = G(D_{a_1,\dots,a_n}, D_{a_1,\dots,a_n}).$$

Lemma 3.3.13. *If* $(a_1,\dots,a_n) > (b_1,\dots,b_n)$*, then*

$$G(D_{a_1,\dots,a_n}, B_{b_1,\dots,b_n}) = 0.$$

Proposition 3.3.14. *We have*

$$\mathcal{B}_n^h = \{B_{a_1,\dots,a_n} \mid (a_1,\dots,a_n) \text{ satisfies the conditions in Remark 3.3.5}\}.$$

Proof. It is easy to see that $|\mathcal{B}_n^h| = |\{B_{a_1,\dots,a_n}\}|$ and $\{B_{a_1,\dots,a_n}\} \subset \mathcal{B}_n^h$. Therefore, it remains to prove that $B_{a_1,\dots,a_n} \neq B_{b_1,\dots,b_n}$ if $(a_1,\dots,a_n) \neq (b_1,\dots,b_n)$. But this follows from the fact that

$$\begin{aligned}\Big(G(B_{a_1,\dots,a_n}, D_{a_1,\dots,a_n}), G(B_{a_1,\dots,a_n}, D_{b_1,\dots,b_n})\Big)&\\ \neq \Big(G(B_{b_1,\dots,b_n}, D_{a_1,\dots,a_n}), G(B_{b_1,\dots,b_n}, D_{b_1,\dots,b_n})\Big)&\end{aligned}$$

by Lemmas 3.3.12 and 3.3.13. □

Now, we can correspond to each element in $\mathcal{B}_n^h$ a n-tuple $(a_1,\dots,a_n)$ and give $\mathcal{B}_n^h$ the same total order as we did on $\mathcal{D}_n^h$. We align the elements in $\mathcal{B}_n^h$ from maximum to minimum. Then we can write B's in term of D's as follows:

$$\begin{pmatrix} B_{1,2,\dots,h,h-1,h,h-1,\dots,h} \\ \vdots \\ B_{1,0,1,0,\dots,1,2,3,\dots,h-1,h} \end{pmatrix} = A \begin{pmatrix} D_{1,2,\dots,h,h-1,h,h-1,\dots,h} \\ \vdots \\ D_{1,0,1,0,\dots 1,2,3\dots,h-1,h} \end{pmatrix},$$

where A is the transform matrix.

Proposition 3.3.15. *We have*

$$A = \begin{pmatrix} 1 & * & \dots & * \\ 0 & 1 & \dots & * \\ \vdots & \vdots & \ddots & \vdots \\ 0 & 0 & \dots & 1 \end{pmatrix}.$$

Proof. The proof follows from Lemma 3.3.12 and Lemma 3.3.13. □

Corollary 3.3.16. *$\mathcal{B}_n^h$ is a basis for $\mathcal{S}(I \times I, n, h)$.*

Proof. As we can see in Corollary 3.3.9, $\mathcal{D}_n^h$ is a basis for $\mathcal{S}(I \times I, n, h)$. By Proposition 3.3.15, the transformation matrix between $\mathcal{B}_n^h$ and $\mathcal{D}_n^h$ is nondegenerate. Therefore, elements in $\mathcal{B}_n^h$ are linearly independent. Moreover, by Proposition 3.2.4, $\mathcal{B}_n^h$ is a generating set. Thus, we have that $\mathcal{B}_n^h$ is a basis of $\mathcal{S}(I \times I, n, h)$. □

3.4 Proof of Main Result

Now we ready to prove our main result, Theorem 5.3.7. We denote the matrix of G with respect to $\mathcal{D}_n^h$ by D. Proposition 3.3.15 gives $\det(B) = \det(D)$. By Corollary 3.3.7 we have $\{D_{a_1,\dots,a_{2n-1}}\}$ is an orthogonal basis with respect to the bilinear form. Thus D is a diagonal matrix with respect to this basis. Therefore,

$$\det(D) = \prod_{(a_1,\dots,a_n)} \langle D_{a_1,\dots,a_n}, D_{a_1,\dots,a_n} \rangle.$$

Thus, by Proposition 3.3.6 we obtain

$$\det(D) = \prod_{(a_1,\dots,a_n)} (\Delta_{a_1} \prod_i \frac{\theta(a_{i+1}, a_i, 1)}{\Delta_{a_{i+1}}}). \tag{3.4.1}$$

In order to simplify the expression $\det(D)$, we need the following lemma which holds immediately from the definitions.

Lemma 3.4.1. *We have*

$$\frac{\theta(a_{i+1}, a_i, 1)}{\Delta_{a_{i+1}}} = \begin{cases} \frac{\Delta_{a_i}}{\Delta_{a_{i+1}}} & \text{if } a_{i+1} = a_i - 1; \\ 1 & \text{if } a_{i+1} = a_i + 1. \end{cases}$$

Lemma 3.4.1 and (3.4.1) give

$$\det(D) = \Delta_h^{|\mathcal{D}_n^h|} \prod_{a_1,\ldots,a_n} (\frac{\Delta_k}{\Delta_{k-1}})^{\alpha^k_{(n,h)}},$$

where $\alpha^k_{(n,h)}$ is the number of times that $\frac{\theta(a_{i+1},a_i,1)}{\Delta_{a_{i+1}}} = \frac{\Delta_k}{\Delta_{k-1}}$. Hence, our problem is reduced to count the number of all such $\frac{\theta(a_{i+1},a_i,1)}{\Delta_{a_{i+1}}}$'s, for a fixed k. To do so, we need the combinatorial structure.

Definition 3.4.2. A lattice path in the plane is a path from $(0,0)$ to (n,h) with northeast and southeast unit steps, where $n \in \mathbb{N}$, and $h \in \mathbb{Z}$. A generalized Dyck path is a lattice path that never goes below the x-axis. We denote the set of all generalized Dyck paths from $(0,0)$ to (n,h) by $\mathcal{D}_{(n,h)}$. We define a-shifted generalized Dyck path to be generalized Dyck path D such that we map each point (x,y) of D to $(x+a, y+a)$. A Dyck path is a generalized Dyck path from $(0,0)$ to $(n,0)$.

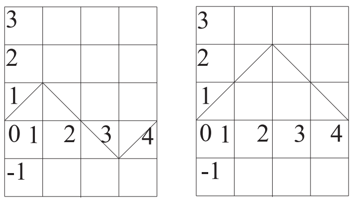

FIGURE 3.6. On the left is a lattice path from $(0,0)$ to $(4,0)$, and on the right is a generalized Dyck path from $(0,0)$ to $(4,0)$

As we can see there is a $1-1$ correspondence between $\mathcal{D}_n^h$ and n-tuples $\{(a_1,\ldots,a_n)\}$ satisfying the conditions in Remark 3.3.5. Note that there is a $1-1$ correspondence between the n-tuples $\{(a_1,\ldots,a_n)\}$ and $(n+1)$-tuples $\{(0,a_1,\ldots,a_n)\}$. Therefore, there is a $1-1$ correspondence between the $(n+1)$-tuples $\{(0,a_1,\ldots,a_n)\}$ and

$\mathcal{D}_{(n,h)}$, for any $(a_1, \ldots, a_n)$ satisfying the conditions in Remark 3.3.5. Hence, there is a $1-1$ correspondence between the sets $\mathcal{D}_n^h$ and $\mathcal{D}_{(n,h)}$, that is, $|\mathcal{D}_n^h| = |\mathcal{D}_{(n,h)}|$.

Definition 3.4.3. A k-down step in a generalized Dyck path is a southeast step from height k to height $k-1$, see Figure 3.7.

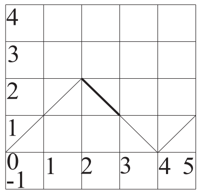

FIGURE 3.7. A 2-down step

Then the problem of counting all $\frac{\theta(a_{i+1}, a_i, 1)}{\Delta_{a_{i+1}}} = \frac{\Delta_k}{\Delta_{k-1}}$ in $\{(a_1, \ldots, a_n)\}$ is equivalent to count all pairs (D, i), where $D \in \mathcal{D}_{(n,h)}$ and $a_i = k, a_{i+1} = k-1$. We denote set of these pairs by $A^k_{(n,h)}$. Geometrically, each pair (D, i) corresponds to a k-down step in the generalized Dyck path D. Counting all pair (D, i) is the same as counting all k-down step in all generalized Dyck path in $\mathcal{D}_{(n,h)}$. The aim of the next section is to count all this kind of steps.

3.5 A combinatorial result

In this section, we are going to prove the following result.

Theorem 3.5.1. *For all n,*

$$\left|A^k_{(n,h)}\right| = \alpha^k_{(n,h)} = \binom{n}{\frac{n+h+2k-2s}{2}} - \binom{n}{\frac{n+h+2k}{2}+1},$$

where $s = \min\{k-1, h\}$.

We prove this theorem by using two different approaches. In Section 3.5.1, we present a combinatorial and geometric explanation, which was inspired by Di Francesco's proof for the case $h = 0$, see [DiF, Proposition 2]. In Section 3.5.2, we present our second approach which is based on the generating function techniques, which provides an alternative proof of Di Francesco's Proposition 2 [DiF].

3.5.1 A geometric proof

In this section, we will construct two maps:

$$\Theta : A^k_{(n,h)} \to \bigcup_{j=0}^{s} \mathcal{D}_{(n,2k-2j+h)} \tag{3.5.1}$$

and

$$\Phi : \bigcup_{j=0}^{s} \mathcal{D}_{(n,2k-2j+h)} \to A^k_{(n,h)}, \tag{3.5.2}$$

where $s = \min\{k-1, h\}$. We will prove that $\Phi\Theta = id$ and $\Theta\Phi = id$. Thus, both of them are bijective. By the reflection principle, we know that

$$|\mathcal{D}_{(n,2k-2j+h)}| = \binom{n}{\frac{n+2k-2j+h}{2}} - \binom{n}{\frac{n+2k-2j+h}{2}+1}. \tag{3.5.3}$$

Therefore,

$$\begin{aligned}\left|\bigcup_{j=0}^{s} \mathcal{D}_{(n,2k-2j+h)}\right| &= \sum_{j=0}^{s} \binom{n}{\frac{n+2k-2j+h}{2}} - \binom{n}{\frac{n+2k-2j+h}{2}+1} \\ &= \binom{n}{\frac{n+h+2k-2s}{2}} - \binom{n}{\frac{n+h+2k}{2}+1}.\end{aligned}$$

Then we have

$$|A^k_{(n,h)}| = \binom{n}{\frac{n+h+2k-2s}{2}} - \binom{n}{\frac{n+h+2k}{2}+1}. \tag{3.5.4}$$

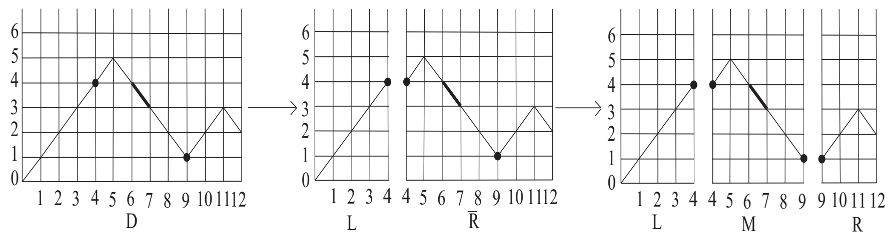

FIGURE 3.8. The cutting process, where $k = 4, n = 12, h = 2, i = 6, l = 9$. The bold step is the one we are considering. Since $a_5 = 5$, we choose $i' = 4$. We cut the path at the 4th place into L and $\bar{R}$. Now, the rightmost lowest point in $\bar{R}$ is $(9, 1)$, so we cut $\bar{R}$ into two parts M and R at $(9, 1)$

Step 1: Construct Θ. Suppose we have a k-down step occurring at the ith place in the Dyck path D. We denote this k-down step by (D, i). We cut D into 3 parts as follows (see Figure 3.8):

1. We choose the largest $i' \leq i$ such that $a_{i'-1} = k-1$ and $a_{i'} = k$, we cut the path at $(i', a_{i'})$. We denote the left part by L, the right part by $\bar{R}$.

2. Now we consider the right part $\bar{R}$. Suppose the lowest height of $\bar{R}$ is j and (l, j) is the lefttmost lowest point of $\bar{R}$. Then we cut $\bar{R}$ at (l, j) into 2 parts. We denote the left part of $\bar{R}$ by M and the right part of $\bar{R}$ by R. One may check that $0 \leq j \leq s$.

Now the path can be considered as a union of 3 parts L, M and R. We do some operations on L, M, R and glue them back as follows (see Figure 3.9):

1. We reflect R with respect to y-axis and shift it down by $h - j$ units. We denote the resulting part by rR. The lowest point of rR is $(n, 2j - h)$. Then by gluing the starting point of rR to the endpoint of M, we get two parts again, L and $M \cup rR$. It is easy to see that the lowest point of $M \cup rR$ is $(n, 2j - h)$.

2. Now we reflect $M \cup rR$ with respect to the y-axis and shift it up by $k - 2j + h$ units. Then we glue it back to the end of L.

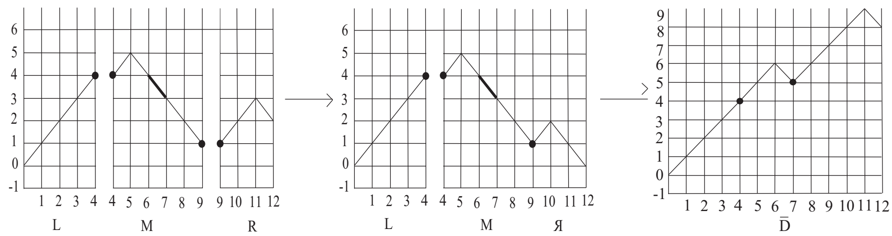

FIGURE 3.9. The glue-back process. We reflect and shift R, we glue it back to M, then we reflect and shift $M \cup rR$ and glue it back to L

At the end, it is easy to see that we have a path $\bar{D} \in \mathcal{D}_{(n,2k-2j+h)}$. We set $\Theta((D, i)) = \bar{D}$, therefore we have established a map

$$\Theta : A^k_{(n,h)} \to \bigcup_{j=0}^{s} \mathcal{D}_{(n,2k-2j+h)}.$$

Step 2: Construct Φ. Basically, this is the reverse process of Θ. Readers can go through Figure 3.8 and Figure 3.9 backward. Suppose we have a path $\bar{D} \in \bigcup_{j=0}^{s} \mathcal{D}_{(n,2k-2j+h)}$. The whole process is as follows:

1. Since the end of $\bar{D}$ is $2k-2j+h > k$, where $0 \leq j \leq s$, there is at least one t such that $a_{t-1} = k-1, a_t = k$ and $a_{t+1} = k+1$. We choose the largest such t, denoted by m, and cut the path $\bar{D}$ at (m, a_m) into two parts L and $r\bar{R}$.

2. By reflecting $r\bar{R}$ and shift it down by $k-2j+h$ units, we obtain a new part $\bar{R}$. The endpoint of $\bar{R}$ is $(n, 2j-h)$.

3. It is easy to see that $y=j$ must intersect $\bar{R}$, since j is always between k and $2j-h$. We choose the leftmost point of $\{y=j\} \cap \bar{R}$ and denote it by (v, a_v). We cut $\bar{R}$ into 2 parts M and rR at (v, a_v).

4. We reflect rR with respect to the y-axis and shift it up by $h-j$ units. We denote the resulting part by R. At the end, we glue the starting point of M to the endpoint of L and glue the beginning point of R to the endpoint of M.

Now we get a Dyck path D from $(0,0)$ to (n,h). We choose the smallest $m' > m$ such that $a_{m'} = k$ and $a_{m'+1} = k-1$. We set $\Phi(\bar{D}) = (D, m')$. Thus, we have established a map

$$\Phi : \bigcup_{j=0}^{s} \mathcal{D}_{(n,2k-2j+h)} \to A_{(n,h)}^{k}.$$

Proposition 3.5.2. *We have $\Phi\Theta = id$ and $\Theta\Phi = id$.*

Proof. Here, we give the detailed proof of the first part of the proposition. The second part is similar. We need to verify that

$$\Phi\Theta : A_{(n,h)}^{k} \to A_{(n,h)}^{k} \tag{3.5.5}$$

is the identity on $A^k_{(n,h)}$. Let us choose an element $(D,i) \in A^k_{(n,h)}$, that is, the k-down step happens at the ith place in the Dyck path $D \in \mathcal{D}_{(n,h)}$. We now apply the process of Θ to (D,i), we get $\bar{D}$, see Figure 3.10. We need find $\Phi(\bar{D})$. Since

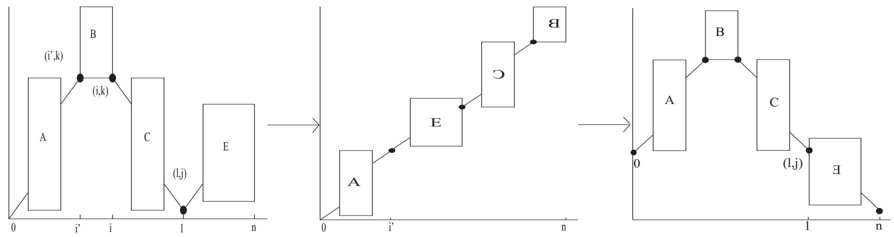

FIGURE 3.10. First, we do construction of Θ, we get $\bar{D}$ as in 3rd diagram from D in 1st diagram. Then we do construction of Φ, we get back from $\bar{D}$ to D in 1st diagram.

in the process of Θ, we shift the path after the i'th place to above the line $y = k$, then the i'th place is the largest t such that $a_{t-1} = k-1, a_t = k, a_{t+1} = k+1$. Thus, $m = i'$. Now, we cut $\bar{D}$ at (m, a_m), then reflect it and glue the resulting path back. It is easy to see that, after the reflection that we did in last step, (l,j) is the leftmost point that we are looking for in step 3 of the process of Φ, i.e. (v, a_v). Then after we cut the path in (l,j), we reflect it and glue the resulting path back, which leads to the path D. In the process of Θ, i' is on the left side of i and is the closest to i satisfying $a_{i'-1} = k-1, a_{i'} = k$. We must choose m' to be on the right side of $m = i'$ and the closest to $m = i'$ satisfying $a_{m'} = k$ and $a_{m'+1} = k-1$. Since $m = i'$, we have that $m' = i$. Therefore $\Theta\Phi((D,i)) = (D,i)$, as required. $\square$

3.5.2 An algebraic proof

Let $C_k(x,q)$ be the generating function for the number of Dyck paths from $(0,0)$ to $(n,0)$ according to the number of steps from height k to height $k-1$, that is,

$$C_k(x,q) = \sum_{n\geq 0} \sum_{p\in\mathcal{D}_{(n,0)}} x^n q^{\#st_k(p)},$$

where $st_k(p)$ denotes the number of steps from height k to height $k-1$ in the path p. Clearly, the generating function for the number of Dyck paths from $(0,0)$ to

$(n, 0)$ is given by

$$C_k(x, 1) = C(x^2) := \frac{1 - \sqrt{1 - 4x^2}}{2x^2}. \tag{3.5.6}$$

Proposition 3.5.3. *The generating function $C_k(x, q)$ is given by*

$$C_k(x, q) = \frac{U_{k-1}\left(\frac{1}{2x}\right) - qxU_{k-2}\left(\frac{1}{2x}\right)C(x^2)}{x\left[U_k\left(\frac{1}{2x}\right) - qxU_{k-1}\left(\frac{1}{2x}\right)C(x^2)\right]},$$

where $C(x^2) = \frac{1-\sqrt{1-4x^2}}{2x^2}$ and U_m is the m-th Chebyshev polynomial of the second kind.

Proof. Since each nonempty Dyck path p in $\mathcal{D}_{n,0}$ can be written as $p = up'dp''$, where p' is any 1-shifted Dyck path and p'' is any Dyck path (u denotes up-step and d denotes down-step), we obtain

$$C_k(x, q) = 1 + x^2 C_{k-1}(x, q) C_k(x, q), \quad k \geq 2 \tag{3.5.7}$$

and

$$C_1(x, q) = 1 + x^2 q C(x^2) C_1(x, q), \tag{3.5.8}$$

where 1 enumerates the path of length zero.

We now proceed the proof by induction on k. Since $U_{-1}(t) = 0$, $U_0(t) = 1$ and $U_1(t) = 2t$, we obtain that (3.5.8) implies that the proposition holds for $k = 1$. Assuming that the claim holds for k, we prove it holds for $k + 1$. Using (3.5.7) together with the induction hypothesis we obtain

$$\begin{aligned}
&C_{k+1}(x, q) \\
&= \frac{1}{1 - x^2 C_k(x, q)} \\
&= \frac{U_k\left(\frac{1}{2x}\right) - qxU_{k-1}\left(\frac{1}{2x}\right)C(x^2)}{U_k\left(\frac{1}{2x}\right) - qxU_{k-1}\left(\frac{1}{2x}\right)C(x^2) - x(U_{k-1}\left(\frac{1}{2x}\right) - qxU_{k-2}\left(\frac{1}{2x}\right)C(x^2))} \\
&= \frac{U_k\left(\frac{1}{2x}\right) - qxU_{k-1}\left(\frac{1}{2x}\right)C(x^2)}{U_k\left(\frac{1}{2x}\right) - xU_{k-1}\left(\frac{1}{2x}\right) - qx(U_{k-1}\left(\frac{1}{2x}\right) - xU_{k-2}\left(\frac{1}{2x}\right))C(x^2))}.
\end{aligned}$$

Using the fact that Chebyshev polynomials $U_m(t)$ of the second kind satisfy the recurrence relation $U_m(t) = 2tU_{m-1}(t) - U_{m-2}(t)$, we get

$$C_{k+1}(x,q) = \frac{U_k\left(\frac{1}{2x}\right) - qxU_{k-1}\left(\frac{1}{2x}\right)C(x^2)}{xU_{k+1}\left(\frac{1}{2x}\right) - qx^2U_k\left(\frac{1}{2x}\right)C(x^2)},$$

which completes the proof. □

Corollary 3.5.4. *[DiF] The number of steps from height k to height $k-1$ in all Dyck paths from $(0,0)$ to $(2n,0)$ is given by*

$$\frac{2k+1}{2n+1}\binom{2n+1}{n+k+1}.$$

Proof. From (3.5.6), (3.5.7) and (3.5.8) we get

$$\frac{d}{dq}C_k(x,q) = x^2C_k(x,q)\frac{d}{dq}C_{k-1}(x,q) + x^2C_{k-1}(x,q)\frac{d}{dq}C_k(x,q)$$

and $\frac{d}{dq}C_1(x,q)\mid_{q=1} = x^2C^3(x^2)$. Hence, by induction on k we have that

$$\frac{d}{dq}C_k(x,q)\mid_{q=1} = x^{2k}C^{2k+1}(x^2). \tag{3.5.9}$$

Since the number of steps from height k to height $k-1$ in all generalized Dyck paths from $(0,0)$ to $(2n,0)$ equals the coefficient of x^{2n} in the generating function $\frac{d}{dq}C_k(x,q)\mid_{q=1}$, we obtain the desired result by [Wilf, Equation 2.5.16]. □

Let $C_{k,h}(x)$ be the generating function for the number of generalized Dyck paths from $(0,0)$ to (n,h) according to the number steps from height k to height $k-1$, that is,

$$C_{k,h}(x,q) = \sum_{n\geq 0}\sum_{p\in\mathcal{D}_{(n,h)}} x^n q^{\#st_k(p)}.$$

In order to an give explicit formula for the generating function $C_{k,h}(x,q)$, we consider the following two cases $k > h$ and $k \leq h$ as follows.

The case $k > h$

In this subsection we fix k where $k > h$. Using the fact that each nonempty generalized Dyck path p in $\mathcal{D}_{n,h}$ can be decomposed as either $p = up'$ where p' is a 1-shifted generalized Dyck path from $(0,0)$ to $(n-1,h-1)$, or $p' = up'dp''$, where p' is a 1-shifted Dyck path from $(0,0)$ to $(n',0)$ and p'' is a generalized Dyck path from $(n'+1,0)$ to (n,h), we obtain

$$C_{k,h}(x,q) = xC_{k-1,h-1}(x,q) + x^2 C_{k-1}(x,q)C_{k,h}(x,q), \quad h \geq 1$$

and

$$C_{k,0}(x,q) = 1 + x^2 C_{k-1}(x,q)C_{k,0}(x,q).$$

By induction on h we get that the generating function $C_{k,h}(x,q)$ which is given by

$$C_{k,h}(x,q) = \frac{x^h}{\prod_{j=k-1-h}^{k-1} 1 - x^2 C_j(x,q)}. \tag{3.5.10}$$

Theorem 3.5.5. *Let $k > h \geq 0$. The number of steps from height k to height $k-1$ in all generalized Dyck paths from $(0,0)$ to (n,h) is given by*

$$\binom{n}{\frac{1}{2}(n-h)+k} - \binom{n}{\frac{1}{2}(n+h)+k+1},$$

where $\binom{a}{b}$ is assumed to be 0 if $a < b$ or if a, b are not nonnegative integers.

Proof. From (3.5.10), we obtain that the number of steps from height k to height $k-1$ in all generalized Dyck paths from $(0,0)$ to (n,h) is given by

$$\begin{aligned}
&[x^n]\left(\frac{d}{dq}C_{k,h}(x,q)\right)_{q=1} \\
&= [x^n]\left[\frac{x^h}{\prod_{j=k-1-h}^{k-1} 1 - x^2 C_j(x,1)} \sum_{j=k-1-h}^{k-1} \frac{x^2 \frac{d}{dq} C_j(x,q) \mid_{q=1}}{1 - x^2 C_j(x,1)}\right],
\end{aligned}$$

which, by (3.5.6) and (3.5.9), is equivalent to

$$[x^n]\left(\frac{d}{dq}C_{k,h}(x,q)\right)_{q=1} = [x^n]\left(x^{h+2}C^{h+2}(x^2)\sum_{j=k-1-h}^{k-1} x^{2j}C^{2j+1}(x^2)\right).$$

Hence, by [Wilf, Equation 2.5.16] we get

$$\begin{aligned}
&[x^n]\left(\frac{d}{dq}C_{k,h}(x,q)\right)_{q=1} \\
&= \sum_{j=k-1-h}^{k-1} \frac{2j+h+3}{n+1}\binom{n+1}{\frac{n-2j-h-2}{2}} \\
&= \sum_{j=k-1-h}^{k-1} \binom{n}{\frac{n-2j-h-2}{2}} - \binom{n}{\frac{n-2j-h-4}{2}} \\
&= \binom{n}{\frac{1}{2}(n-h)+k} - \binom{n}{\frac{1}{2}(n+h)+k+1}
\end{aligned}$$

as claimed. In the second equality, we use

$$\binom{n}{k} - \binom{n}{k-1} = \frac{n-2k+1}{n+1}\binom{n+1}{k}. \tag{3.5.11}$$

□

The case $k \le h$

In this subsection we fix k where $k \le h$. Using similar arguments as discussed in the above subsection we get that the generating function $C_{k,h}(x,q)$ satisfies

$$C_{k,h}(x,q) = xC_{k-1,h-1}(x,q) + x^2 C_{k-1}(x,q)C_{k,h}(x,q), \quad h \ge 1$$

and

$$C_{0,h}(x,q) = xC_{0,h-1}(x,q) + x^2 C(x^2)C_{0,h}(x,q).$$

By induction on h we get $C_{0,h}(x,q) = x^h C^{h+1}(x^2)$, which, by induction on k, implies that

$$C_{k,h}(x,q) = \frac{x^h C^{h-k+1}(x^2)}{\prod_{j=0}^{k-1} 1 - x^2 C_j(x,q)}. \tag{3.5.12}$$

Theorem 3.5.6. *Let $1 \le k \le h$. The number of steps from height k to height $k-1$ in all generalized Dyck paths from $(0,0)$ to (n,h) is given by*

$$\binom{n}{\frac{n+h}{2}+1} - \binom{n}{\frac{n+h}{2}+k+1},$$

where $\binom{a}{b}$ is assumed to be 0 if $a < b$ or if a, b are not nonnegative integers.

Proof. From (3.5.12), we obtain that the number of steps from height k to height $k-1$ in all generalized Dyck paths from $(0,0)$ to (n,h) is given by

$$\begin{aligned}
&[x^n]\left(\frac{d}{dq}C_{k,h}(x,q)\right)_{q=1} \\
&= [x^n]\left[\frac{x^h C^{h-k+1}(x^2)}{\prod_{j=0}^{k-1} 1-x^2C_j(x,1)}\sum_{j=0}^{k-1}\frac{x^2\frac{d}{dq}C_j(x,q)\mid_{q=1}}{1-x^2C_j(x,1)}\right],
\end{aligned}$$

which, by (3.5.6) and (3.5.9), is equivalent to

$$[x^n]\left(\frac{d}{dq}C_{k,h}(x,q)\right)_{q=1} = [x^n]\left(x^{h+2}C^{h+3}(x^2)\sum_{j=0}^{k-1}x^{2j}C^{2j}(x^2)\right).$$

Hence, by [Wilf, Equation 2.5.16] we obtain

$$\begin{aligned}
&[x^n]\left(\frac{d}{dq}C_{k,h}(x,q)\right)_{q=1} \\
&= \sum_{j=0}^{k-1}\frac{h+2j+3}{n+1}\binom{n+1}{\frac{n-2j-h-2}{2}} \\
&= \sum_{j=0}^{k-1}\binom{n}{\frac{n-2j-h-2}{2}} - \binom{n}{\frac{n-2j-h-4}{2}} \\
&= \binom{n}{\frac{n+h}{2}+1} - \binom{n}{\frac{n+h}{2}+k+1}
\end{aligned}$$

as claimed. In the second equality, we use the Equation 3.5.11. □

3.6 A new semi-meander determinant

Di Francesco [DiF] defined a *semi-meander determinant*. Here, we will present a different bilinear form on the same module. We will calculate the Gram determinant of this new form with respect to a natural basis.

Definition 3.6.1. [DiF] A semi-meander of order n with winding number h is a planar configuration of non-selfintersecting loops crossing the positive half line through n distinct points and negative half line through h distinct points such that no two points from the set of h points are contiguous on a loop. We consider such diagrams up to smooth deformations preserving the topology of the configuration.

We can cut the semi-meander into an upper and a lower diagram as described in Figure 3.11.

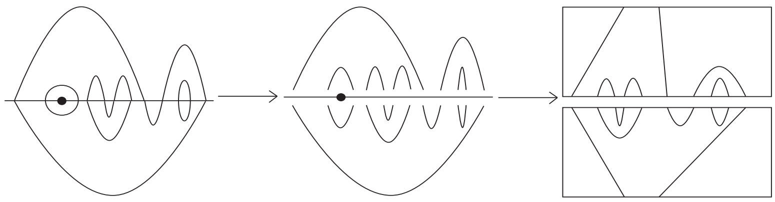

FIGURE 3.11. A semi-meander of order $n = 10$ with winding number $h = 2$

Definition 3.6.2. Let $B'_{a_1,\ldots,a_n}$ be the diagram $B_{a_1,\ldots,a_n}$ with the idempotent on a_n removed. We denote $\mathcal{E}_n^h$ to be $span_\Lambda\{B'_{a_1,\ldots,a_n}\}_{(a_1,\ldots,a_n)} \subset \mathcal{S}(I \times I, n+h)$.

Di Francesco [DiF] defined the following matrix:

Definition 3.6.3. [DiF] $T = [T_{a,b}]$ with $T_{a,b} = \delta^{c(a,b)}$, where $a, b \in \{B'_{a_1,\ldots,a_n}\}_{(a_1,\ldots,a_n)}$ and $c(a,b)$ is the number of the components of the semimeander by gluing a to b.

Remark 3.6.4. We can define a bilinear form on $\mathcal{E}_n^h$ by extending the map $f(a,b) = \delta^{c(a,b)}$ with $a, b \in \{B'_{a_1,\ldots,a_n}\}_{(a_1,\ldots,a_n)}$ bilinearly. The matrix T defined by Di Francesco is the matrix of this bilinear form with respect to the basis $a, b \in \{B'_{a_1,\ldots,a_n}\}_{(a_1,\ldots,a_n)}$.

Now, we define a different matrix as follows:

Definition 3.6.5. Let $S = [S_{a,b}]$ with $S_{a,b} = \delta^{c(a,b)}$, where $a, b \in \{B'_{a_1,\ldots,a_n}\}_{(a_1,\ldots,a_n)}$, and $c(a,b)$ is the number of the components of the semi-meander obtained by gluing a to b if the h intersection points on the negative half line belong to h distinct components of the resulting collection of loops; otherwise, $S_{a,b}$ is 0.

Theorem 3.6.6. *We have*

$$\det(S) = (\frac{\Delta_1^h}{\Delta_h})^{|\mathcal{D}_n^h|}\det(B) = \Delta_1^{|\mathcal{D}_n^h|}\prod_k(\frac{\Delta_k}{\Delta_{k-1}})^{\alpha^k_{(n,h)}}.$$

Proof. Let $\mathcal{E}_n^h$ be the subspace of $\mathcal{S}(D^2, n+h)$ defined in Definition 3.6.2. Just as in TL_n, we define a map L on $\{B'_{a_1,\ldots,a_n}\}_{(a_1,\ldots,a_n)} \times \{B'_{a_1,\ldots,a_n}\}_{(a_1,\ldots,a_n)}$ by connecting two elements in $\{B'_{a_1,\ldots,a_n}\}_{(a_1,\ldots,a_n)}$ with $n+h$ parallel strings. If the h points on $I \times \{1\}$ belong to h different components, then we evaluate the resulting diagram by Kauffman bracket. Otherwise, we make it 0. Then we extend this map to a bilinear form on $\mathcal{E}_n^h$. It is easy to see that the matrix of L with respect to the basis $\{B'_{a_1,\ldots,a_n}\}_{(a_1,\ldots,a_n)}$ is equal to S. Moreover,

$$G(B_{(a_1,\ldots,a_n)}, B_{(b_1,\ldots,b_n)}) = \frac{\Delta_1^h}{\Delta_h} L(B'_{(a_1,\ldots,a_n)}, B'_{(b_1,\ldots,b_n)}),$$

for all $(a_1,\ldots,a_n),(b_1,\ldots,b_n)$. Then the result follows easily from Theorem 5.3.7.

□

Chapter 4

Mahler Measure of Colored Jones Polynomials

4.1 Introduction

The Volume Conjecture suggests that values of the colored Jones polynomials of a knot converges to the volume of the knot complement in some way. The conjecture is a hard problem to solve. Thus some mathematicians want to see whether some measure of colored Jones polynomial of certain sequence of knots converge. The Mahler measure [Sk] in a sense is the canonical measure of complexity on the space of complex polynomials. In [CK], Champanerkar and Kofman prove that the Mahler measure of Jones polynomials of a certain sequence of knots generated from a fixed knot converges. In this chapter, we adapt their methods to show a more general result by using a basis of generalized Temperley-Lieb algebra, which will be introduced below.

4.2 Generalized Temperley-Lieb Algebra and A Special Subspace

In Chapter 3, we define the colored skein module and study one generalization of Temperley-Lieb algebra. In this chapter, we generalize the Temperley-Lieb algebra in another way and investigate the relation between these algebras and colored Jones polynomials.

Definition 4.2.1. The $n \times i$ generalized Temperley-Lieb algebra $GTL(n, i)$ is the colored skein module of $I \times I$ with $2n$ points on boundary and each colored by i.

Remark 4.2.2. The nth Temperley-Lieb Algebra TL_n is a special case of the $n \times i$ generalized Temperley-Lieb algebra $GTL(n, i)$ with $i = 1$.

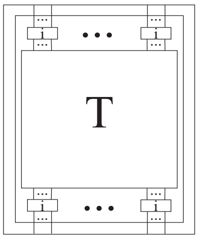

FIGURE 4.1. Consider an element in $GTL(n, i)$ as an element in $TL_{n\times i}$.

We also need consider the natural pairing on $TL_{n\times i}$, which is discussed in Chapter 2.

Definition 4.2.3. Define the pairing

$$< R, S >=< R\hat{S} >$$

where $\hat{S}$ means we reflect the skein element S with respect to vertical line, $R\hat{S}$ means we gluing them together at two ends with $n \times i$ non-intersecting arcs and $<>$ means we use Kauffman bracket to evaluate the diagram.

We also remind reader of a property from Chapter 2.

Proposition 4.2.4. *This pairing on $TL_{n\times i}$ is non-degenerate.*

4.3 A Graph Basis Of $GTL(n, i)$

In Chapter 2, an orthogonal basis is constructed for Temperley-Lieb algebra. In this section, we will build a similar basis for generalized Temperley-Lieb algebra.

Definition 4.3.1. Let $D^i_{a_1,\ldots,a_{2n-1}}$ be the element of $GTL(n, i)$ in the Figure 4.2, where a_i satisfies:

1. $a_1 = a_{2n-1} = i$;
2. $a_k \in \mathbb{N}$ for all k;
3. (a_k, a_{k-1}, i) is admissible for all k.

Let $\mathfrak{D}(n, i)$ be the collection of all these D's.

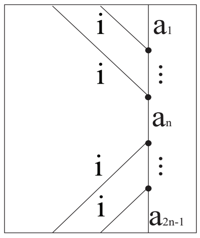

FIGURE 4.2. At each black dot, the graph is admissible.

We have a nice formula for inner product of basis elements with respect to the natural pairing.

Lemma 4.3.2. *Suppose* $(a_1, ..., a_{2n-1})$ *and* $(b_1, ..., b_{2n-1})$ *satisfy all the conditions above, then*

$$\begin{aligned} &< D^i_{a_1,...,a_{2n-1}}, D^i_{b_1,...,b_{2n-1}} > \\ = \;& \delta_{a_1,b_1}\Delta_{a_{2n-1}} \prod_{j=1}^{2n-2} [\delta_{a_{j+1},b_{j+1}} \frac{\theta(a_{j+1}, a_j, i)}{\Delta_{a_{j+1}}}] \end{aligned}$$

Moreover, it is easy to see that it is nonzero when $(a_1, \cdots, a_{2n-1}) = (b_1, \cdots, b_{2n-1})$.

Proof. We prove the formula by induction.

When $n = 2$, by and direct computation,

$$\begin{aligned} &< D^i_{a_1,a_2,a_3}, D^i_{b_1,b_2,b_3} > \\ = \;& \Delta_{a_3}\delta_{a_1b_1}\delta_{a_2b_2}\delta_{a_3b_3} \frac{\theta(a_2, a_1, i)}{\Delta_{a_2}} \frac{\theta(a_3, a_2, i)}{\Delta_{a_3}}. \end{aligned}$$

Thus the formula is true for $n = 2$. Now suppose the formula is true for $n = k - 1$ and let $n = k$.

$$\begin{aligned} &< D^i_{a_1,...,a_{2n-1}}, D^i_{b_1,...,b_{2n-1}} > \\ = \;& \delta_{a_1b_1}\delta_{a_{2n-1}b_{2n-1}} \frac{\theta(a_2, a_1, i)}{\Delta_{a_2}} \frac{\theta(a_{2n-1}, a_{2n-2}, i)}{\Delta_{a_{2n-2}}} < D^i_{a_2,...,a_{2n-2}}, D^i_{b_2,...,b_{2n-2}} > \\ = \;& \delta_{a_1b_1}\delta_{a_{2n-1}b_{2n-1}} \frac{\theta(a_2, a_1, i)}{\Delta_{a_2}} \frac{\theta(a_{2n-1}, a_{2n-2}, i)}{\Delta_{a_{2n-2}}} \times \\ & \delta_{a_2b_2}...\delta_{a_{2n-2}b_{2n-2}} \frac{\theta(a_3, a_2, i)}{\Delta_{a_3}} \cdots \frac{\theta(a_{2n-2}, a_{2n-3}, i)}{\Delta_{a_{2n-2}}} \Delta_{a_{2n-2}} \\ = \;& \Delta_{a_{2n-1}}\delta_{a_1b_1}...\delta_{a_{2n-1}b_{2n-1}} \frac{\theta(a_2, a_1, i)}{\Delta_{a_2}} \cdots \frac{\theta(a_{2n-1}, a_{2n-2}, i)}{\Delta_{a_{2n-1}}}. \end{aligned}$$

Thus the formula holds for $n = k$. Hence, by induction, the formula holds. $\square$

Corollary 4.3.3. *$D^i_{a_1,\cdots,a_{2n-1}}$'s are linearly independent.*

Proof. This follows easily from Lemma 4.3.2. $\square$

Lemma 4.3.4. *The identity in $GTL(n,i)$ can be written as linear combination of $D^i_{a_1,\cdots,a_{2n-1}}$'s.*

Proof. We prove the result by induction.

For $n = 2$, the result follows from the fusion identity as in Figure 4.3. We just need

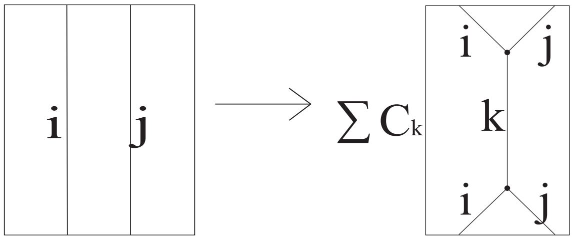

FIGURE 4.3. Fusion.

take $i = j$. Now suppose the result is true for $n = k$, we need prove the case for $n = k$. We choose two rightmost string and do the fusion as the first step in Figure 4.4. Then we use induction to the circled part of the second diagram in Figure 4.4 and rearrange the diagram, we obtain the last diagram in Figure 4.4. $\square$

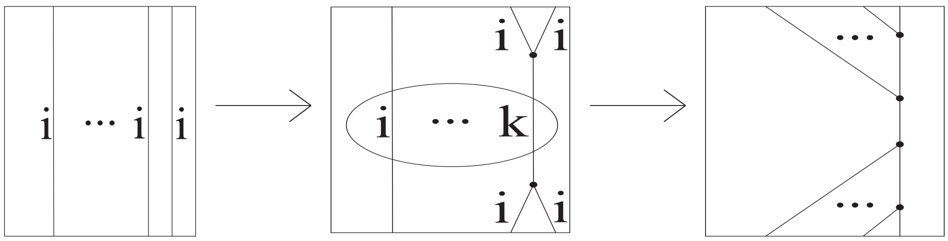

FIGURE 4.4. Induction step.

Lemma 4.3.5. *Any element in $GTL(n,i)$ can be written as linear combination of $D^i_{a_1,\cdots,a_{2n-1}}$'s.*

Proof. We will show the proof diagrammatically. We choose a small neighborhood of n colored points on the two ends and use two identities. By Lemma 4.3.4, we can write them as linear combination of $D_{a_1,\cdots,a_{2n-1}}$'s as in Figure 4.5. Now consider the middle box of the second diagram in Figure 4.5. We can consider it as an element in $\mathcal{S}(I \times I, 2)$ with two points on the boundary colored. It is well known that the skein module $\mathcal{S}(I \times I, 2)$ with two points on the boundary colored is either 0 dimension or 1 dimension with basis to be corresponding idempotent. Therefore, we can write the element in middle box to be a constant times an idempotent. Then we can simplify the element as in second step in Figure 4.5. That mean each element can be written as linear combination of $D_{a_1,\cdots,a_{2n-1}}$. $\square$

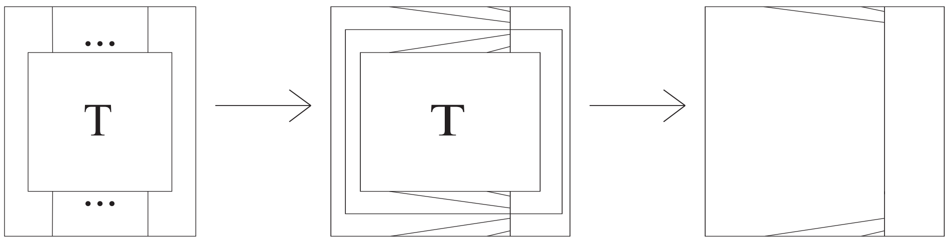

FIGURE 4.5.

Theorem 4.3.6. $\{D^i_{a_1,\cdots,a_{2n-1}}\}$ *is a basis of* $GTL(n,i)$.

Proof. By Corollary 4.3.3 and Lemma 4.5, $D^i_{a_1,\cdots,a_{2n-1}}$'s are linearly independent and they span the whole space. Therefore, they are a basis for $GTL(n,i)$. $\square$

Remark 4.3.7. Patrick Gilmer also prove that $\{D^i_{a_1,\cdots,a_{2n-1}}\}$ is a basis in [G5] by decompose any skein element in $GTL(n,i)$ into union of 3-balls with 3 colored points on the boundary.

Theorem 4.3.8. *We have* $D^i_{a_1,\cdots,a_{2n-1}}$ *is an eigenvector of full twist action with eigenalue* $(-1)^{a_n}A^{a_n^2+2a_n}$.

Proof. This follows from the calculation in the proof of [Li6, Lemma 14.1]. $\square$

4.4 Symmetric Basis Elements

In this section, we consider some elements in the basis constructed in Section 4.3.

Definition 4.4.1. A basis element $D^i_{a_1,\cdots,a_{2n-1}}$ is called symmetric if

$$a_j = a_{2n-j}$$

for all j.

We can normalize these symmetric elements.

Definition 4.4.2. Suppose

$$d_{a_1,\cdots,a_n} = \prod_{j=1}^{n-1} \frac{\theta(a_{j+1}, a_j, i)}{\Delta_{a_{j+1}}}.$$

We define

$$G^i_{a_1,\cdots,a_n} = D^i_{a_1,\cdots,a_{n-1},a_n,a_{n-1},\cdots,a_1}/d_{a_1,\cdots,a_n}$$

Proposition 4.4.3. *The normalized symmetric elements are orthogonal idempotents in $GTL(n,i)$, that is, we have*

$$G^i_{a_1,\cdots,a_n} G^i_{b_1,\cdots,b_n} = \delta_{a_1,b_1} \cdots \delta_{a_n,b_n} G^i_{a_1,\cdots,a_n}$$

Proof. This follows from direct computation. □

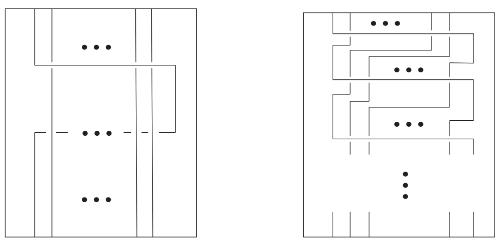

FIGURE 4.6. S_n and F_n.

Remark 4.4.4. We denote the left in Figure 4.6 by S_n, and the right by F_n.

If we color each component of S_n or F_n in Figure 4.6 with ith Jones-Wenzl idempotent, we obtain two elements in $GTL(n,i)$, denoted by S^i_n or F^i_n. Next, we will show some property of S^i_n and F^i_n.

Proposition 4.4.5. *We have*

$$S_n^i = \sum c_{a_1\cdots,a_n} G^i_{a_1\cdots,a_n}.$$

where

$$c_{a_1\cdots,a_n} = A^{2a_{n-1}+2i-2a_n+a_{n-1}^2+i^2-a_n^2}$$

Proof. Since $\{D^i_{a_1,\cdots,a_{2n-1}}\}$ form a basis for $GTL(n,i)$, then we have

$$S_n^i = \sum s_{a_1,\cdots,a_{2n-1}} D^i_{a_1,\cdots,a_{2n-1}}.$$

Applying the bilinear pairing to $GTL(n,i)$, it is easy to see that

$$s_{a_1,\cdots,a_{2n-1}} =< S_n^i, D^i_{a_1,\cdots,a_{2n-1}} > / < D^i_{a_1,\cdots,a_{2n-1}}, D^i_{a_1,\cdots,a_{2n-1}} > .$$

By Lemma 4.3.2, we have

$$< D^i_{a_1,\cdots,a_{2n-1}}, D^i_{a_1,\cdots,a_{2n-1}} >= \Delta_{a_n}(d_{a_1,\cdots,a_n})^2$$

Moreover, by [KL, Proposition 3, Lemma 7], we have

$$\begin{aligned} &< S_n^i, D^i_{a_1,\cdots,a_{2n-1}} > \\ &= A^{2a_{n-1}+2i-2a_n+a_{n-1}^2+i^2-a_n^2} \Delta_{a_n} \prod_{j=1}^{n-1} \delta_{a_j a_{2n-j}} \prod_{j=1}^{n-1} \frac{\theta(a_{j+1}, a_j, i)}{\Delta_{a_{j+1}}} \end{aligned}$$

So

$$s_{a_1,\cdots,a_{2n-1}} = \begin{cases} A^{2a_{n-1}+2i-2a_n+a_{n-1}^2+i^2-a_n^2} \prod_{j=1}^{n-1} \frac{\Delta_{a_{j+1}}}{\theta(a_{j+1},a_j,i)} & \text{if } a_j = a_{2n-j} \text{ for all } j \\ 0 & \text{otherwise} \end{cases}$$

Since

$$G^i_{a_1,\cdots,a_n} = D^i_{a_1,\cdots,a_{n-1},a_n,a_{n-1},\cdots,a_1} / d_{a_1,\cdots,a_n}$$

and

$$d_{a_1,\cdots,a_n} = \prod_{j=1}^{n-1} \frac{\theta(a_{j+1}, a_j, i)}{\Delta_{a_{j+1}}},$$

we have

$$S_n^i = \sum c_{a_1\cdots,a_n} G^i_{a_1\cdots,a_n}.$$

where

$$c_{a_1\cdots,a_n} = A^{2a_{n-1}+2-2a_n+a_{n-1}^2+1-a_n^2}.$$

□

Proposition 4.4.6. *We have*

$$F_n^i = \sum e_{a_1\cdots,a_n} G^i_{a_1\cdots,a_n}.$$

where

$$e_{a_1\cdots,a_n} = (-1)^{a_n} A^{a_n^2+2a_n}$$

Proof. If we concatenate F_n^i with $G^i_{a_1\cdots,a_n}$, we can move all twists in F_n^i over to $G^i_{a_1\cdots,a_n}$. As a result, we get a diagram with the middle segment of $G^i_{a_1\cdots,a_n}$ fully twisted. According to [Li6, Lemma 14.1], we get the result. □

4.5 Colored Jones Polynomial And Mahler Measure

There are various ways to define colored Jones polynomial. We take Jone-Wenzl idempotent and Kauffman bracket way. By coloring a link with the nth Jones-Wenzl idempotents one may use the Kauffman bracket to compute the nth colored Jones polynomial as follows:

Definition 4.5.1. The ith colored Jones polynomial of link L is defined to be

$$J_i(L) = A^{-(k^2+2k)w(L)} < L(i) > .$$

Here $L(i)$ is the link L with each component colored by f_i, $<>$ is the Kauffman bracket and $w(L)$ is the writhes of L.

Next we give the definition of Mahler measure.

Definition 4.5.2. Let $f \in \mathbb{C}[z_1^{\pm 1}, \cdots, z_k^{\pm 1}]$. The Mahler measure of f is defined to be

$$M(f) = e^{\int_0^1 \cdots \int_0^1 \log |f(e^{2\pi i \theta_1} \cdots e^{2\pi i \theta_k})| d\theta_1 \cdots d\theta_k}$$

In this paper, we will mainly use the following theorem about Mahler measure.

Theorem 4.5.3. *[La] For every $f \in \mathbb{C}[z_1^{\pm 1}, \cdots, z_k^{\pm 1}]$,*

$$M(f) = \lim_{u \to \infty} M(f(z, z^u, \cdots, z^{u^k})).$$

Given link L, we can construct a sequences of links based on L by cutting L along n strands and adding in m copies of element X in TL_n. We call the new link LX_m. For example, one could use X as the elements of TL_n given in Figure 4.6.

In the case of F_n, if we cut L along n strings, we obtain a tangle in $I \times I$ with $2n$ endpoints and we denote it by L_n. We can consider it as an element in TL_n. If we stack m copies of F_n on top of L_n and close the new tangle up, we get the new links, denoted by LF_m. We will consider the ith colored Jones polynomial of LF_m. In [CK], the following theorem is proved.

Theorem 4.5.4. *The Mahler measure of ith colored Jones polynomial of LF_m converges to the Mahler measure of a 2-variable polynomial as m goes to infinity. That is*

$$\lim_{m \to \infty} M(J_i(LF_m)) = M(P_i(x, y))$$

for some $P_i \in \mathbb{C}[x^{\pm 1}, y^{\pm 1}]$

They used the commutative property of full twist. We will use the basis of $GTL(n, i)$ constructed here to prove a more general theorem. In particular, we can show that above theorem is true for both LS_m and LF_m.

4.6 Application Of Graph Basis

In this section, we will prove the following theorem.

Theorem 4.6.1. *The Mahler measure of ith colored Jones polynomial of LX_m converges to the Mahler measure of a 2-variable polynomial as m goes to infinity when X is a tangle in TL_n and*

$$X = \sum a_{a_1,\cdots,a_n} G_{a_1,\cdots,a_n},$$

where a_i's are monomials of A. That is

$$\lim_{m\to\infty} M(J_i(LX_m)) = M(P_i(x,y)).$$

for some $P_i \in \mathbb{C}[x^{\pm 1}, y^{\pm 1}]$. Here J_i is the ith colored Jones polynomial.

Proof. First, we cut $LX_m(i)$ into two pieces with one piece L_n^i and the other piece $(X^i)^m$, here L_n^i means that each component of L_n is colored with f_i and $(X^i)^m$ means the concatenation of m copies of X^i. Then by definition of the pairing, we have

$$< LX_m(i) >=< L_n^i, (X^i)^m > .$$

Since

$$X^i = \sum a_{a_1,\cdots,a_n} G^i_{a_1\cdots,a_n},$$

then

$$(X^i)^m = (\sum a_{a_1\cdots,a_n} G^i_{a_1\cdots,a_n})^m.$$

But we know that $G^i_{a_1\cdots,a_n}$'s are orthogonal to each other, we have

$$(X^i)^m = \sum (a_{a_1\cdots,a_n})^m (G^i_{a_1\cdots,a_n})^m.$$

Then by Property 4.4.3, we have

$$(X^i)^m = \sum (a_{a_1\cdots,a_n})^m G^i_{a_1\cdots,a_n}.$$

So by the linearity of the pairing, the Kauffman bracket of LX_m is

$$< LX_m(i) >=< L_n^i, (X^i)^m >= \sum (a_{a_1 \cdots, a_n})^m < L_n^i, G^i_{a_1 \cdots, a_n} > .$$

Let

$$< L_n^i, G^i_{a_1 \cdots, a_n} >= Q(A), a^m_{a_1, \cdots, a_n} = R_{a_1, \cdots, a_n}(A^m)$$

Now we can define

$$P_i(x, y) = \sum Q(x)R(y).$$

then we have

$$P_i(A, A^m) =< LX_m(i) > .$$

According to the definition of Mahler measure, it is easy to see that Mahler measures of two functions differing by a monomial are the same. We have

$$M(J_i(LX_m)) = M(< LX_m(i) >).$$

Then by applying Theorem 4.5.3 we get

$$\lim_{m \to \infty} M(J_i(LX_m)) = \lim_{m \to \infty} M(P_i(A, A^m)) = M(P_i(x, y)).$$

□

Corollary 4.6.2. *The Theorem 4.6.1 is true for $X = S, F$.*

Proof. This follows from Proposition 4.4.5 and Proposition 4.4.6. □

Chapter 5
Turaev-Viro Endomorphism

5.1 Introduction

5.1.1 History

Walker first noticed [Wa1] that the endomorphism induced in a $2+1$-TQFT (defined over a field) by the exterior of a closed off Seifert surface of a knot in zero-framed surgery along the knot can be used to give lower bounds for the genus of the knot. He did this by showing the number of non-zero eigenvalues of this endomorphism counted with multiplicity is an invariant [Wa1], i.e. it does not depend on the choice of the Seifert surface. Thus the number of such eigenvalues must be less than or equal to the dimension of the vector space that the TQFT assigns to a closed surface of this minimal genus.

Next Turaev and Viro [TV], again assuming the TQFT is defined over a field, saw that the similarity class of the induced map on the vector space associated to a Seifert surface modulo the generalized 0-eigenspace was a stronger invariant. If the TQFT is defined over a more general commutative ring, the second author observed that the strong shift equivalence class of the endomorphism is an invariant of the knot [G3]. Strong shift equivalence (abbreviated SSE) is a notion from symbolic dynamics which we will discuss in §5.2.4 below. For a TQFT defined over a field F, the similarity class considered by Turaev-Viro is a complete invariant of SSE. In this case, the vector space modulo the generalized 0-eigenspace together with the induced automorphism, considered as a module over $F[t, t^{-1}]$, is called the Turaev-Viro module. It should be considered as somewhat analogous to the Alexander module. The order of the Turaev-Viro module is called the Turaev-Viro polynomial and lies in $F[t, t^{-1}]$. We will refer to the endomorphisms constructed as above (and those in the same SSE class) as Turaev-Viro endomorphisms.

In [G1, G2], Turaev-Viro endomorphisms were studied and methods for computing the endomorphism explicitly were given. These methods adapted Rolfsen's surgery technique of studying infinite cyclic covers of knots. This method requires finding a surgery description of the knot; that is a framed link in the complement of the unknot such that the framed link describes S^3 and the unknot represents the original knot. Moreover each of the components of the framed link should have linking number zero with the unknot. For this method to work, it is important that the surgery presentation have a nice form. In this chapter, we will show that all knots have a surgery presentations of this form (in fact an even nicer form that we will call standard.) Another explicit method of computation was given by Achir, and Blanchet [AB]. This method starts with any Seifert surface. The second author also considered the further invariant obtained by decorating a knot with a colored meridian (this was needed to give formulas for the Turaev-Viro endomorphism of a connected sum, and to use the Turaev-Viro endomorphism to compute the quantum invariants of branched cyclic covers of the knot).

Ohtsuki [O1, O2] arrived at the same invariant as the Turaev-Viro polynomial but from a very different point of view. Ohtsuki extracts this invariant from a surgery description of a knot (alternatively of a closed 3-manifold with a primitive one dimensional cohomology class) and the data of a modular category. His method starts from any surgery description standard or not. This is a significant advantage of his approach. Ohtsuki's proof of the invariance of the polynomial in [O1] is only sketched. He stated that his invariant is the same as the Turaev-Viro polynomial, but does not give an explanation.

Recently Viro has returned to these ideas [V1, V2]. He has studied the Turaev-Viro endomorphism of a knot after coloring both the meridian and the longitude of the knot. Viro observed that a weighted sum of the traces of these endomorphisms is the colored Jones polynomial evaluated at a root of unity.

In [G1, G2, G3], Turaev-Viro endomorphisms were defined more generally for infinite cyclic cover of 3-manifolds. Suppose (M, χ) is a closed connected oriented 3-manifold M with $\chi \in H^1(M, \mathbb{Z})$ such that $\chi : H_1(M, \mathbb{Z}) \to \mathbb{Z}$ is onto. Let M_∞ be the infinite cyclic cover of M corresponding to χ. Choose a surface Σ in M dual to χ. By lifting Σ to M_∞, we obtain a fundamental domain E with respect to the action of $\mathbb{Z}$ on M_∞. E is a cobordism from a surface Σ to itself.Let (V, Z) be a $2+1$-TQFT on the cobordism category of extended 3-manifolds and extended surfaces. Applying (V, Z) to E and Σ, we can construct an endomorphism $Z(E) : V(\Sigma) \to V(\Sigma)$. In [G3], it is proved that the strong shift equivalent class of $Z(E) : V(\Sigma) \to V(\Sigma)$ is an invariant of the pair (M, χ), i.e. it does not depend on the choice of Σ. We denote this SSE class by $\mathcal{Z}(M, \chi)$. We will sometimes refer to a pair (M, χ) as above, informally, as a 3-manifold with an infinite cyclic covering.

The knot invariants discussed above can be obtained as special cases of the above invariants of 3-manifolds with an infinite cyclic covering. For any *oriented* knot K in S^3, we obtain an extended 3-manifold $S^3(K)$ by doing 0-surgery along K. We choose χ to be the integral cohomology class that evaluates to 1 on a positive meridian of K. Then it is easy to see that the invariant $\mathcal{Z}(S^3(K), \chi)$ corresponding to $(S^3(K), \chi)$ only depends on K. If our TQFT is defined for 3-manifolds with colored links, one may obtain further invariants by coloring the meridian and the longitude (a little further away) of the knot.

For the knot invariants discussed above, it is required, in general, that K is oriented. [1] This is so that the exterior of a Seifert surface acquires a direction as a cobordism from the Serfert surface to itself. However, we decided to delay mentioning this technicality. To avoid issues that arise from phase anomalies in TQFT, in this chapter, we work with extended manifolds as in [Wa2] and [T]. In this introduction, we omit mentiona of the integer weights and lagrangian subspaces of extended manifolds. We discuss extended manifolds carefully in main text.

5.1.2 Results of this chapter

Inspired by Ohtsuki, we construct a SSE class $Z(M, \chi)$ from a framed (or banded) tangle in $S^2 \times I$ that arises in a surgery presentation of (M, χ). We call this the tangle endomorphism. Moreover we show that the endomorphism (or square matrix) that Ohtsuki considers in this situation is well defined up to SSE. By relating the definition of the Turaev-Viro endomorphism to Ohtsuki's matrix, we give a different proof of the invariance of Ohtsuki's invariant. In fact, we show that Ohtsuki's matrix has the same SSE class as the Turaev-Viro endomorphism, i.e. $\mathcal{Z}(M, \chi) = Z(M, \chi)$. We do not prove these results in the general case of a TQFT arising from a modular category. We only work in the context of the skein approach for TQFTs associated to $SO(3)$ and $SU(2)$. We work with a modified Blanchet-Habegger-Masbaum-Vogel approach [BHMV2] as outlined in [GM2]. This theory is defined over a slightly localized cyclotomic ring of integers. It is worthwhile studying endomorphisms defined up to strong shift equivalence over this ring rather than passing to a field. We show that the traces of the Turaev-Viro endomorphism of knots with the meridian and longitude colored turns out to encode exactly the same information as the colored Jones polynomial evaluated at a root of unity.

[1] For TQFTs over a field satisfying some common axioms, the Turaev-viro endomorphisms of a knot and its inverse have the same SSE class. This follows from [G1, Proposition 1.5] and Proposition 5.2.23.

5.1.3 Organization of this chapter

In section 5.2, we discuss extended manifolds, a variant of the TQFT constructed in [BHMV2], surgery presentations and the definition of SSE. In section 5.3, we construct an endomorphism for each framed tangle in $S^2 \times I$ and apply it to the tangle obtained from a surgery presentation of an infinite cyclic cover of a 3-manifold. We call it the tangle endomorphism. Then we state Theorem 5.3.7 which states that the SSE class of a tangle endomorphism constructed from a surgery presentation of (M, χ) is an of invariant (M, χ). In section 5.4, we discuss technical details concerning the Turaev-Viro endomorphism for (M, χ), and the method of calculating $\mathscr{Z}(M, \chi)$ introduced in [G1, G2]. In section 5.5, we relate the tangle endomorphism associated to a nice surgery presentation to the corresponding Turaev-Viro endomorphism. In section 5.6, we prove Theorem 5.3.7. In section 5.7, we give formulas relating the colored Jones polynomial to the traces of Turaev-Viro endomorphism of a knot whose meridian and longitude are colored. In section 5.8, we compute two examples to illustrate these ideas.

5.1.4 Convention

All surfaces and 3-mainifolds are assumed to be oriented.

5.2 Preliminaries

5.2.1 Extended surfaces and extended 3-manifolds.

For each integer $p \geq 3$, Blanchet, Habegger, Masbaum and Vogel define a TQFT from quantum invariants of 3-manifolds at $2p$th root of unity over a 2+1-cobordism category in [BHMV2]. The cobordism category has surfaces with p_1-structures as objects and 3-manifolds with p_1-structures as morphisms. They introduce p_1-structures in order to resolve the framing anomaly. Following [G4, GM2], we will adapt the theory by using extended surfaces and extended 3-manifolds in [Wa2, T] instead of p_1-structures to resolve the framing anomaly. In the following, all homology groups have rational coefficients except otherwise stated.

Definition 5.2.1. An extended surface $(\Sigma, \lambda(\Sigma))$ is a closed surface Σ with a lagrangian subspace $\lambda(\Sigma)$ of $H_1(\Sigma)$ with respect to its intersection form, which is a symplectic form on $H_1(\Sigma)$.

Definition 5.2.2. An extended 3-manifold $(M, r, \lambda(\partial M))$ is a 3-manifold with an integer r, called its weight, and whose oriented boundary ∂M is given an extended surface structure with lagrangian subspace $\lambda(\partial M)$. If M is a closed extended 3-manifold, we may denote the extended 3-manifold simply by (M, r).

Remark 5.2.3. Suppose we have an extended 3-manifold $(M, r, \lambda(\partial M))$ and $\Sigma \subset \partial M$ is a closed surface. Then

$$\lambda(\partial M) \cap H_1(\Sigma)$$

need not be a lagrangian subspace of $H_1(\Sigma)$.

Definition 5.2.4. Suppose we have an extended 3-manifold $(M, r, \lambda(\partial M))$ and $\Sigma \subset \partial M$ is a closed surface. If $\lambda(\partial M) \cap H_1(\Sigma)$ is a lagrangian subspace of $H_1(\Sigma)$, we call Σ equipped with this lagrangrian a boundary surface of the extended 3-manifold $(M, r, \lambda(\partial M))$.

Notation 5.2.5. If Σ is a surface, we use $\bar{\Sigma}$ to denote the surface Σ with the opposite orientation.

Proposition 5.2.6. *Suppose (V_1, ω_1) and (V_2, ω_2) are two symplectic vector spaces. Consider the symplectic vector space $V_1 \oplus V_2$ with symplectic form $\omega_1 \oplus \omega_2$. We can identify V_1 and V_2 as symplectic subspaces of $V_1 \oplus V_2$. If $\lambda \subset V_1 \oplus V_2$ is a lagrangian subspace such that $\lambda \cap V_1$ is a lagrangian subspace of V_1, then $\lambda \cap V_2$ is a lagrangian subspace of V_2.*

Proof. Since $\lambda \cap V_1 = \text{span} < a_1, \cdots, a_n >$ where $n = \frac{1}{2}\text{dim}(V_1)$, we can assume that

$$\lambda = \text{span} < (a_1, 0), \cdots, (a_n, 0), (c_1, b_1), \cdots, (c_m, b_m) >,$$

where $m = \frac{1}{2}\text{dim}V_2$. Since for any i, j

$$\begin{aligned} 0 &= \omega_1 \oplus \omega_2((a_i, 0), (c_j, b_j)) \\ &= \omega_1(a_i, c_j) + \omega(0, b_j) \\ &= \omega_1(a_i, c_j), \end{aligned}$$

we have $c_j \in (\lambda \cap V_1)^\perp = \lambda \cap V_1$. Therefore,

$$\lambda = \text{span} < (a_1, 0), \cdots, (a_n, 0), (0, b_1), \cdots, (0, b_m) > .$$

That means $\text{dim}(\lambda \cap V_2) = m$. So $\lambda \cap V_2$ is a lagrangian subspace in V_2. □

Corollary 5.2.7 ([GM2])**.** *Suppose we have an extended* 3*-manifold* $(M, r, \lambda(\partial M))$ *and* $\Sigma \subset \partial M$ *is a boundary surface. Then* $\partial M - \Sigma$*, equipped with the lagrangian* $H_1(\partial M - \Sigma) \cap \lambda(\partial(M))$*, is also a boundary surface.*

Proof. This follows from Proposition 5.2.6. □

In the next three definitions, we describe the morphisms and the composition of morphisms in $\mathcal{C}$, a cobordism category whose objects are extended surfaces.

Definition 5.2.8. Let $(M, r, \lambda(\partial M))$ be an extended 3-manifold. Suppose

$$\partial M = \bar{\Sigma} \cup \Sigma',$$

and this boundary has been partitioned into two boundary surfaces $\bar{\Sigma}$, called (minus) the source, and Σ', called the target. We write

$$(M, r, \lambda(\partial M)) : (\Sigma, \lambda(\bar{\Sigma})) \to (\Sigma', \lambda(\Sigma')),$$

and call $(M, r, \lambda(\partial M))$ an extended cobordism.

Definition 5.2.9. Let Σ be a boundary surface of an extended 3-manifold $(M, r, \lambda(\partial M))$ with inclusion map

$$i_{\Sigma,M} : \Sigma \to M.$$

Let Σ' be $\partial M - \Sigma$ with inclusion map

$$i_{\Sigma',M} : \Sigma' \to M.$$

Then we define

$$\lambda_M(\Sigma) = i_{\Sigma,M}^{-1}(i_{\Sigma',M}(\lambda(\Sigma'))).$$

We define the composition of morphisms in $\mathcal{C}$ as the extended gluing of cobordisms.

Definition 5.2.10. Let $(M, r, \lambda(\partial M))$ and $(M', r', \lambda(\partial M'))$ be two extended 3-manifolds. Suppose $(\Sigma, \lambda(\Sigma))$ is a boundary surface of $(M, r, \lambda(\partial M))$ and $(\bar{\Sigma}, \lambda(\Sigma))$ is a boundary surface of $(M', r', \lambda(\partial M'))$. Then we can glue $(M, r, \lambda(\partial M))$ and $(M', r', \lambda(\partial M'))$ together with the orientation reversing identity from Σ to $\bar{\Sigma}$ to form a new extended 3-manifold. The new extended 3-manifold has

1. base manifold: $M \cup_\Sigma M'$

2. lagrangian subspace:

$$[\lambda(\partial M) \cap H_1(\partial M - \Sigma)] \oplus [\lambda(\partial M') \cap H_1(\partial M' - \bar{\Sigma})],$$

3. weight:

$$r + r' - \mu(\lambda_M(\Sigma), \lambda(\Sigma), \lambda_{M'}(\bar{\Sigma})),$$

   where μ is the Maslov index as in [T].

Definition 5.2.11. Let $(M, r, \lambda(\partial M))$ be an extended 3-manifold with a boundary surface of the form $\Sigma \cup \bar{\Sigma}$. Then we define the extended 3-manifold obtained by gluing Σ and $\bar{\Sigma}$ together to be the extended 3-manifold that results from gluing $(M, r, \lambda(\partial M))$ and $(\Sigma \times [0,1], 0, \lambda(\Sigma \cup \bar{\Sigma}))$ along $\Sigma \cup \bar{\Sigma}$. In the special case that $\partial M = \Sigma \cup \bar{\Sigma}$, we call the resulting extended 3-manifold the closure of $(M, r, \lambda(\partial M))$.

Remark 5.2.12. One should think of the weight of an extended 3-manifold M as the signature of some background 4-manifold [Wa2]. See also [G4, p. 399].

Lemma 5.2.13. *Let $(R, r, \lambda(\partial R))$ be a morphism from $(\Sigma, \lambda(\Sigma))$ to $(\Sigma', \lambda(\Sigma'))$ and $(S, s, \lambda(\partial S))$ be a morphism from $(\Sigma', \lambda(\Sigma'))$ to $(\Sigma, \lambda(\Sigma))$. Then the extended 3-manifold we obtain by gluing $(R, r, \lambda(\partial R))$ to $(S, s, \lambda(\partial S))$ along Σ' first and then closing it up along Σ is the same as the one we obtained from gluing $(S, s, \lambda(\partial S))$ to $(R, r, \lambda(\partial R))$ along Σ first and then closing it up along Σ'.*

Proof. This can be seen from the 4-manifold interpretation of weights in [Wa2, GM2]. □

Extended surfaces may also be equipped with banded points: this is an embedding of the disjoint union of oriented intervals. By a framed link, we will mean what is called a banded link in [BHMV2, p.884], i.e. an embedding of the disjoint union of oriented annuli. Framed 1-manifold are defined similarly. Extended 3-manifolds are sometimes equipped with framed links, or framed 1-manifolds or more generally trivalent fat graphs. By a trivalent fat graphs, we will mean what is called a banded graph in [BHMV2, p.906]. The framed links, framed 1-manifolds and trivalent fat graphs must meet the boundary surfaces of a 3-manifold in banded points with the induced "banding". Of course, we could have used the word "banded" in all cases, but the other terminology is more common.

There is a surgery theory for extended 3-manifolds. We refer the reader to [GM2, §2]. Here we give extended version of Kirby moves [K]. These moves relate framed links in S^3 where S^3 is itself equipped with an integer weight. The result of extended surgery of S^3 with its given weight along the link is preserved by these moves. Moreover (but we do not use this) if surgery along two framed links in weighted copies of S^3 result in the same extended manifold then there is sequence of extended Kirby moves relating them.

Definition 5.2.14. The extended Kirby-1 move is the regular Kirby-1 move with weight of manifold changed accordingly. More specifically, if we add an ϵ-framed unknot to the surgery link, then we change the weight of the manifold by $-\epsilon$, where $\epsilon = \pm 1$. If we delete an ϵ-framed unknot from the surgery link, then we change the weight of the manifold by ϵ. The extended Kirby-2 move is the regular Kirby-2 move with the weight remaining the same.

5.2.2 A variant of the TQFT of Blanchet, Habegger, Masbaum and Vogel.

Suppose a closed connected 3-manifold M is obtained from S^3 by doing surgery along a framed link L, then (M, r) is obtained from $(S^3, r-\sigma(L))$ by doing extended surgery along L. Here $\sigma(L)$ is the signature of the linking matrix of L. Warning this is different than the signature of L . The quantum invariant of (M, r) at a $2p$th root of unity A is then defined as:

$$Z((M,r)) = \eta \kappa^{r-\sigma(L)} < L(\omega) >,$$

where

$$\Delta_k =< U(e_k) >, \quad \eta^{-1} = \sqrt{\sum_k \Delta_k^2}, \quad \omega = \sum_k \eta \Delta_k e_k, \quad \kappa =< U_+(\omega) > .$$

We use $< >$ to denote the Kauffman bracket evaluation of a linear combination of colored links in S^3, and $\mathcal{L}(x)$ to denote the satellization of a framed link $\mathcal{L}$ by a skein x of the solid torus. Moreover e_k denotes the skein class in the solid torus obtained by taking the closure of f_k, the Jones-Wenzl idempotent in the k-strand

Temperley-Lieb algebra. Here U denotes the zero framed unknot and U_+ is the unknot with framing $+1$. The sum is over the colors $0 \le k \le p/2 - 2$ if p is even and $0 \le k \le p - 3$ with k even if p is odd. One has that κ is a square root of $A^{-6-p(p+1)/2}$. The choice of square root here determines the choice in the square root in the formula of η^{-1}, or vice-versa. See the formula for η in [BHMV2, page 897]. The closed connected manifold M may also have an embedded p-admissibly colored fat trivalent graph G in the complement of the surgery, then

$$Z((M,r),G) = \eta\kappa^{r-\sigma(L)} < L(\omega) \cup G > .$$

By following the exactly the same procedure in [BHMV2], we can construct a TQFT for the category of extended surfaces and extended 3-manifolds from quantum invariants. The TQFT assigns to each extended surface $(\Sigma, \lambda(\Sigma))$, possibly with some banded colored points, a module $V(\Sigma, \lambda(\Sigma))$ over $k_p = \mathbb{Z}[\frac{1}{p}, A, \kappa]$, and assigns to each extended cobordism M, with a p-admissibly colored trivalent fat graph meeting the banded colored points,

$$(M, r, \lambda(M)) : (\Sigma, \lambda(\Sigma)) \to (\Sigma', \lambda(\Sigma'))$$

a k_p-module homomorphism:

$$Z((M, r, \lambda(M))) : V((\Sigma, \lambda(\Sigma)) \to V((\Sigma', \lambda(\Sigma'))).$$

Then by using this TQFT, we can produce a Turaev-Viro endomorphism associated to each weighted closed 3-manifold equipped with a choice of infinite cyclic cover using the procedure described in §5.1.

Notation 5.2.15. We introduce some notations that will be used later.

1. $\Lambda_k^{(l)} = \eta^l \Delta_k^l f_k$,

2. $\omega^{(l)} = \sum_k \eta^l \Delta_k^l e_k$,

3. $\Theta(a, b, c)$ is the Kauffman bracket of the left diagram in Figure 5.1,

4. $Tet(a, b, c, d, e, f)$ is the Kauffman bracket of the right diagram in Figure 5.1.

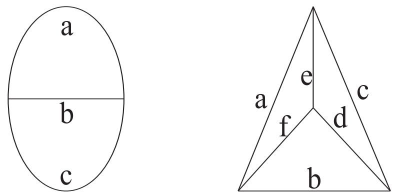

FIGURE 5.1. On the left is $\Theta(a, b, c)$, and on the right is $\mathrm{Tet}(a, b, c, d, e, f)$.

5.2.3 Surgery presentations

The earliest use of surgery presentations, that we are aware of, was by Rolfsen [R2] to compute and study the Alexander polynomial. In this chapter we consider surgery descriptions for extended closed 3-manifolds with an infinite cyclic cover. We will use these descriptions for extended 3-manifolds that contain certain colored trivalent fat graphs. As this involves no added difficulty, we will not always mention these graphs in this discussion.

Definition 5.2.16. Let $K_0 \cup L$ be a framed link inside (S^3, s) where K_0 is an oriented 0-framed unknot, and the linking numbers of the components of L with K_0 are all zero. Let D_0 be a disk in S^3 with boundary K_0 which is transverse to L. Suppose (M, r) is the result of extended surgery along $K_0 \cup L$, then there exists a unique epimorphism $\chi : H_1(M, \mathbb{Z}) \to \mathbb{Z}$ which agrees with the linking number with K_0 on cycles in $S^3 \setminus (K_0 \cup L)$. We will call (D_0, L, s) a surgery presentation of $((M, r), \chi)$. We remark that, in this situation, we will have $s = r - \sigma(L)$. If there are graphs G' in M and G in $S^3 \setminus (K_0 \cup L)$ (transverse to D_0) related by the surgery, we will say (D_0, L, s, G) a surgery presentation of $((M, r), \chi, G')$.

If the result of surgery along L returns S^3 with the image of K_0 after surgery becoming a knot oriented knot K, and the linking numbers of the components of

L with K_0, then $K_0 \cup L$ is a surgery presentation of K as in Rolfsen. The manifold obtained by surgery along $K_0 \cup L$ in S^3 is the same as 0-framed surgery along K in S^3.

The following Proposition is proved in section 4 of [O1] for non-extended manifolds. The extended version involves no extra difficulty

Proposition 5.2.17. *Every extended connected* 3*-manifold with an epimorphism* $\chi : H_1(M, \mathbb{Z}) \to \mathbb{Z}$ *has a surgery presentation.*

Every surgery presentation can be described by diagram as in Figure 5.2 which we will refer to as a surgery presentation diagram.

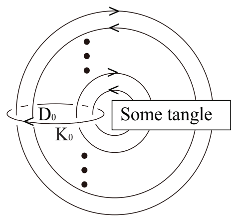

FIGURE 5.2. A surgery presentation diagram. Of course, the tangle must be such that each closed component of L has zero linking number with K_0. Notice the orientation on K_0.

Definition 5.2.18. If a surgery presentation diagram is in the form of Figure 5.3, then we say this surgery presentation diagram is in standard form. We will also say that a surgery presentation (D_0, L, s, G) is standard if it has a surgery presentation diagram in standard form.

Ohtsuki [O1, bottom of p. 259] stated a proposition about surgery presentations of knots which is similar to the following proposition. Our proof is similar to the proof that Ohtsuki indicated. We will call a Kirby-1 move in a surgery presentation a small Kirby-1 move if a disk which bounds the created or deleted component is in the complement of D_0. We will call a Kirby-2 move in a surgery presentation a small Kirby-2 move if it involves sliding a component other than K_0 over another

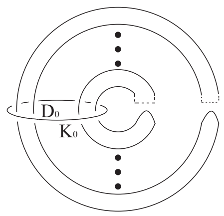

FIGURE 5.3. The dotted part could be knotted or linked with other strands within the tangle box. The bottom turn-backs are simple arcs without double points under the projection. Each component of L intersects the flat disc D_0 bounded by the trivial knot algebraically 0 times, but geometrically 2 times.

component that is in the complement of D_0. A D_0-move is a choice of a new spanning disk D' with $D_0 \cap D' = K_0$ followed by an ambient isotopy that moves D' to the original position of D_0 and moves L at the same time.

Proposition 5.2.19. *A surgery presentation described by a surgery presentation diagram can be transformed into a surgery presentation described by a surgery presentation diagram in standard form by a sequence of isotopies of $L \cup G$ relative to D_0, small Kirby-1 moves, small Kirby-2 moves, and D_0-moves. Therefore, every extended 3-manifold with an epimorphism $\chi : H_1(M, \mathbb{Z}) \to \mathbb{Z}$ has a standard surgery presentation.*

Proof. We need to prove that we can change a surgery presentation described by a surgery diagram as in Figure 5.2 into surgery presentation described by a diagram as in Figure 5.3 using the permitted moves.

Let

$$m = \max_{L_i \text{ is a component of } L} |L_i \cap D_0|.$$

We will prove the theorem by induction on m. Since each component L_i has linking number 0 with K_0, it is easy to see that m is even.

If $m = 0$, then L can be taken to be contained in the tangle box.

When $m = 2$, we may

- first do a D_0 move to shift D_0 slightly;
- then perform an isotopy relative to the new D_0 of L so that the points on intersection of the image of the old D_0 with each components of L are adjacent to each other;
- then do another D_0-move to move the old D_0 back to its original position.

Now the arcs emitted from the bottom edge of the tangle are in a correct order. But the diagram in Figure 5.2 may differ from a standard tangle in the way that the arcs emitted from bottom edge of the tangle box are not in the specified simple form. This means they could be knotted and linked with each other. However we may perform small Kirby-1 and small Kirby-2 moves as in Figure 5.4 to unknot and unlink these arcs so that the resulting diagram has standard form.

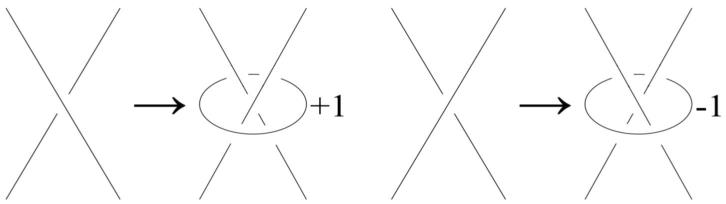

FIGURE 5.4. We use $+1$ or -1 surgery on unknot to change the crossing.

We now prove that the theorem holds for all links with $m = 2n$ where $n \geq 2$, assuming it holds for all links with $m \leq 2n - 2$. Suppose the component L_1 intersects D_0 geometrically $2n$ times. Because L_1 has linking number 0 with K_0, we have that at least one arc, say α of L_1 in Figure 5.2 which joins two points on the bottom of the tangle box, i.e. it is a "turn-back". For each crossing with exactly one arc from α, we can make the arc α to be the top arc (in the direction perpendicular to the plane of the diagram) by using the moves of Figure 5.4, which just involve some small Kirby-1 and small Kirby-2 moves. Then it is only simply linked to other components by some new trivial components with framing ±1. Then by using isotopies relative to D_0, we can slide the arc α towards bottom of the tangle, with the newly created unknots stretched vertically in the diagram so that they intersect each horizontal cross-section in at most 2-points. See the central illustration Figure 5.5 where α is illustrated by two vertical arcs meeting a small box labeled X. This small box contains the rest of α. Now perform a D_0 move which has the effect of pulling the turn-back across D_0. Those trivial components will follow the turn back and pass through D_0. But since at the beginning, those components have geometric intersection 0 with D_0, they have geometric intersection 2 with D_0 now. After this process, $L_1 \cap D_0$ is reduced by two. This process does not change the number of intersections with D_0 of the other components of the original L.

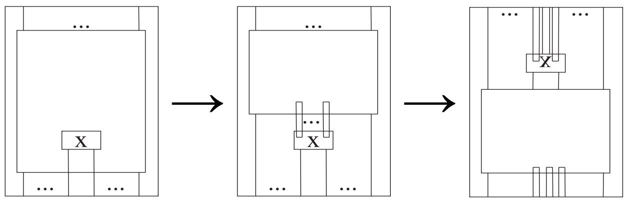

FIGURE 5.5. Moves which reduce the number of intersections of a component of L with D_0. We perform small K-moves and isotopies to change to the middle picture. We perform a D_0-move to change to the right hand picture.

We do this process for all components L_j with $|L_j \cap D_0| = 2n$. Then the new link has $m \leq 2n-2$. By our induction hypothesis, we can transform $K_0 \cup L$ into a standard form using the allowed moves. $\square$

5.2.4 Strong shift equivalence.

We will discuss SSE in the category of free finitely generated modules over a commutative ring with identity. This notion arose in symbolic dynamics. For more information, see [Wag, LM] and references therein.

Definition 5.2.20. Suppose

$$X : V \to V, Y : U \to U$$

are module endomorphisms. We say X is elementarily strong shift equivalent to Y if there are two module morphisms

$$R : V \to U, S : U \to V$$

such that

$$X = SR, Y = RS.$$

We denote this by $X \approx Y$.

Definition 5.2.21. Suppose

$$X : V \to V, Y : U \to U$$

are module endomorphisms. We say X is strong shift equivalent to Y if there are finite number of module endomorphisms $\{X_1, ..., X_n\}$ such that

$$X \approx X_1 \approx X_2 ... \approx X_n \approx Y.$$

We denote this by $X \sim Y$.

It is easy to see that if $X \sim Y$, then $\mathrm{Trace}(X) = \mathrm{Trace}(Y)$.

Proposition 5.2.22. *Let X be a module endomorphism of V. Suppose $V = U \oplus W$ where U and W are free finitely generated modules such that U in the kernel of X, and let $\hat{X}$ be the induced endomorphism of W, then $\hat{X}$ is SSE to X.*

Proof. Suppose $\mathrm{Rank}(U) = m$, and $\mathrm{Rank}(W) = n$. The result follows from the following block matrix equations.

$$\left[\begin{array}{c} v_{m\times n} \\ \hline \hat{X}_{n\times n} \end{array}\right]_{(n+m)\times n} \cdot \left[\begin{array}{c|c} 0_{n\times m} & I_n \end{array}\right]_{n\times(n+m)} = \left[\begin{array}{c|c} 0_{m\times m} & v_{m\times n} \\ \hline 0_{n\times m} & \hat{X}_{n\times n} \end{array}\right]_{(n+m)\times(n+m)}$$

$$\left[\begin{array}{c|c} 0_{n\times m} & I_n \end{array}\right]_{n\times(n+m)} \cdot \left[\begin{array}{c} v_{m\times n} \\ \hline \hat{X}_{n\times n} \end{array}\right]_{(n+m)\times n} = \left[\hat{X}_{n\times n}\right]_{n\times n}$$

□

If T is an endomorphism of a vector space V, let $N(T)$ denote the generalized 0-eigenspace for T, and $T_\flat$ denote the induced endomorphism on $V/N(T)$. The next proposition may be deduced from more general statements made in [BH, p. 122, Prop(2.4)]. For the convenience of the reader, we give direct proof.

Proposition 5.2.23. *Let T and T' be endomorphisms of vector spaces. T and T' are SSE if and only if $T_\flat$ and $T'_\flat$ are similar.*

Proof. The only if implication is well-known [LM, Theorem 7.4.6]. The if implication follows from the easy observations that similar transformations are strong shift equivalent and that T is strong shift equivalent to $T_\flat$. This second fact follows from the repeated use of the following observation: If $x \neq 0$ is in the null space of T, $< x >$ denotes the space spanned by x, and T_x denotes the induced map on $V/ < x >$, then T and T_x are strong shift equivalent. This follows from Proposition 5.2.22 with $U =< x >$. □

5.3 The tangle morphism

In this section, we will assign a k_p-module homomorphism to any framed tangle in $S^2 \times I$ enhanced with an embedded p-admissibly colored trivalent fat graph in the complement of the tangle. By slicing a surgery presentation for an infinite cyclic cover of an extended 3-manifold and applying the TQFT, we obtain such a tangle, and thus a k_p-module endomorphism. The idea of constructing this endomorphism is inspired by the work of Ohtsuki in [O1].

There is a unique lagrangian for a 2-sphere. Thus we can consider any 2-sphere as an extended manifold without specifying a lagrangian. Similarly, we let $(S^2 \times I, r)$ denote the extended manifold $S^2 \times I$ with weight r, as there is no need to specify a lagrangian.

Definition 5.3.1. Let S be a 2-sphere equipped with m ordered uncolored banded points, and u ordered banded points colored by $x_1, \cdots, x_u$. We define $S(i_1, i_2, \cdots i_m)$ to be this 2-sphere where the m uncolored banded points have been colored by $(i_1, i_2, \cdots i_m)$ (and the u points already colored remain colored).

We define

$$V(S) = \sum_{i_1,\ldots,i_m} V(S(i_1, i_2, \cdots i_m)).$$

Here $V(S(i_1, i_2, \cdots i_m))$ is the module for a extended 2-sphere with m uncolored banded points colored by $(i_1, \cdots, i_m)$ and u banded points colored by $(x_1, \cdots, x_u)$ obtained by applying the TQFT that we introduced in §5.2.

By an (m, n)-tangle in $(S^2 \times I, r)$, we mean a properly embedded framed 1-manifold in $(S^2 \times I, r)$ with m endpoints on $S_0 = S^2 \times \{0\}$, n points on $S_1 = S^2 \times \{1\}$, with possibly some black dots on its components and a (possibly empty) colored trivalent fat graph (in the complement of the 1-manifold) meeting S_0 in u colored points $x_1, \cdots, x_u$ and meeting S_1 in t colored points $y_1, \cdots, y_t$. Thus S_0 is a 2-sphere with m ordered uncolored banded points and u colored banded points. Similarly S_1 is a 2-sphere with n ordered uncolored banded points and t colored banded points. For any (m, n)-tangle, we will define a homomorphism from $V(S_0)$ to $V(S_1)$.

Before doing that, we introduce some definitions. From now on, we will not explicitly mention the banding on the selected points of a surface or the framing of a tangle, or the fattening of a trivalent graph. Each comes equipped with such and the framing/fattening of a link/graph induces the banding on its boundary points. Nor will we mention the ordering chosen for uncolored sets of points.

Definition 5.3.2. Suppose we have a (m, n)-tangle in $(S^2 \times I, r)$ with a colored trivalent graph with u edges colored by $x_1, \cdots, x_u$ meeting $S^2 \times \{0\}$ and t edges colored by $y_1, \cdots, y_t$ meeting $S^2 \times \{1\}$. Suppose we color the m endpoints from the tangle on $S_0 = S^2 \times \{0\}$ by $i_1, \cdots, i_m$ and color the n endpoints from the tangle on $S_1 = S^2 \times \{1\}$ by $j_1, \cdots, j_n$. We say that the coloring $(i_1, \cdots, i_n, j_1, \cdots, j_m)$ is legal if the two endpoints of the same strand have the same coloring. We denote the tangle with the endpoints so-colored by $T^{n,(j_1,\ldots,j_n)}_{m,(i_1,\ldots,i_m)}$. For an example, see Figure 5.6.

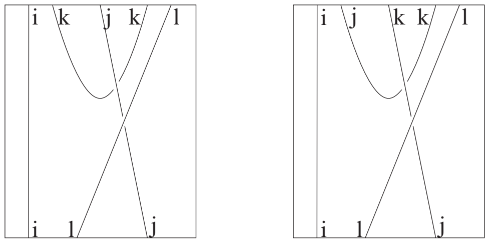

FIGURE 5.6. The coloring in first diagram is a legal coloring and the one in the second diagram is a illegal coloring for $k \neq j$. In this example, the colored trivalent graph is empty.

Definition 5.3.3. Suppose we have $T^{n,(j_1,\ldots,j_n)}_{m,(i_1,\ldots,i_m)}$, a $(i_1, \cdots, i_m, j_1, \cdots, j_n)$ colored (m, n)-tangle as in Definition 5.3.2. We define a homomorphism

$$V(S_0(i_1, \cdots, i_m)) \overset{Z(T^{n,(j_1,\ldots,j_n)}_{m,(i_1,\ldots,i_m)})}{\longrightarrow} V(S_1(j_1, \cdots, j_n))$$

as follows.

- If $(i_1, \cdots, i_m, j_1, \cdots, j_n)$ is a illegal coloring. We take the homomorphism to be the zero homomorphism.
- If $(i_1, \cdots, i_m, j_1, \cdots, j_n)$ is a legal coloring. We decorate uncolored components of the tangle by some skeins in two cases:
    1. If there are l black dots on the component, $l \in \{0, 1, 2, \cdots\}$, and the component has two endpoints with color k, $k \in \{i_1, \cdots, i_m, j_1, \cdots, j_n\}$, then we decorate the component by $\Lambda^{(l)}_k$.

2. If there are l black dots on the component, $l \in \{0, 1, 2, \cdots\}$, and the component lies entirely in $S^2 \times (0, 1)$, then we decorate the component by $\omega^{(l)}$.

Then we apply Z to $(S^2 \times I, r)$ with the tangle T_m^n, so decorated, to get the morphism $Z(T_{m,(i_1,\ldots,i_m)}^{n,(j_1,\ldots,j_n)})$.

Now we are ready to define the homomorphism for a tangle T_m^n.

Definition 5.3.4. Suppose we have a (m, n)-tangle T_m^n. We define the homomorphism for the tangle, denoted by $Z(T_m^n)$, to be

$$V(S_0) \xrightarrow{\sum Z(T_{m,(i_1,\ldots,i_m)}^{n,(j_1,\ldots,j_n)})} V(S_1)$$

where $Z(T_{m,(i_1,\ldots,i_m)}^{n,(j_1,\ldots,j_n)})$ is as in Definition 5.3.3 and the sum runs over all colorings $(i_1, \cdots, i_m, j_1, \cdots, j_n)$.

Proposition 5.3.5. *For a tangle T_1 in $(S^2 \times I, r)$ and a tangle T_2 in $(S^2 \times I, s)$, we have*

$$Z(T_2 \circ T_1) = Z(T_2)Z(T_1),$$

where $T_2 \circ T_1$ in $(S^2 \times I, r + s)$ means gluing T_2 on the top of T_1. Here, of course, we assume that the top of T_1 and the bottom of T_2 agree.

Proof. This follows from the functoriality of the original TQFT. □

Now we can construct tangle endomorphisms for an extended closed 3-manifold with an embedded colored trivalent graph, and choice of infinite cyclic cover. Given $((M, r), \chi, G')$, we choose a surgery presentation (D_0, L, s, G). We put one black dot somewhere on each component of L away from D_0. By doing a 0-surgery along K_0, we obtain $(S^2 \times S^1, s)$ with link L and trivalent graph G, where D_0 can be completed to $S^2 \times \{p\}$ for some point p on S^1. We cut $S^2 \times S^1$ along $S^2 \times \{p\}$. Then we obtain a tangle $\mathcal{T}_n^n$ in $(S^2 \times I, s)$. Here $n = |\mathcal{T}_n^n \cap (S^2 \times \{1\})| = |\mathcal{T}_n^n \cap (S^2 \times \{0\})|$. Let $Z(\mathcal{T}_n^n)$ denote tangle endomorphism associated to $\mathcal{T}_n^n$.

Lemma 5.3.6. *If $\mathcal{T}_n^n$ is constructed as above, then the SSE class of $Z(\mathcal{T}_n^n)$ is independent of the positioning of the black dots.*

Proof. By definition, we can move a black dot on the component of the tangle $\mathcal{T}_n^n$ anywhere without changing the tangle endomorphism $Z(\mathcal{T}_n^n)$. We move the black dot to near bottom or near top and cut the tangle $\mathcal{T}_n^n$ into two tangles S and T, where T is a trivial tangle with the black dot. For an example, see Figure 5.7. Then we switch the position of S and T and move the black dot in resulting tangle to near the other end of that component. Then we do the process again. By doing this, we can move it to any arc of the tangle $\mathcal{T}_n^n$, which belongs to the same component of the link L. But for each step, $Z(ST) = Z(S)Z(T)$ is strong shift equivalent to $Z(TS) = Z(T)Z(S)$. Therefore, the lemma is true. $\square$

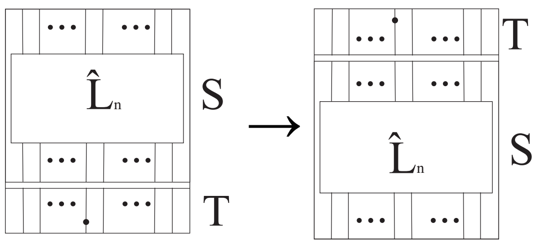

FIGURE 5.7. Here T is the trivial part with the black dot.

Thus the SSE class of the tangle endomorphism $Z(\mathcal{T}_n^n)$ constructed as above depends only on a surgery presentation (D_0, L, s, G). Thus we can denote this class by $Z(D_0, L, s, G)$.

Theorem 5.3.7. *Let (D_0, L_1, s_1, G_1) and (D_0, L_2, s_2, G_2) be two surgery presentations for $((M, r), \chi, G')$, an extended closed 3-manifold with an embedded colored* *trivalent graph, and choice of infinite cyclic cover. Then*

$$Z(D_0, L_1, s_1, G_1) = Z(D_0, L_2, s_2, G_2).$$

Thus we may denote this SSE class by $Z((M, r), \chi, G')$.

This theorem will be proved in section 5.6, after the way has been prepared in sections 5.4 and, 5.5.

5.4 The Turaev-Viro endomorphism

In §5.1, we introduced the basic idea of the Turaev-Viro endomorphism. In this section, we will include the technical details.

Remark 5.4.1. The discussion in this section and the next section works for 3-manifolds with an embedded p-admissibly colored trivalent graph. For simplicity, we usually omit mention of the trivalent graph. Thus we will write $((M, r), \chi)$ instead of $((M, r), \chi, G')$. This is according to the philosophy that we should think of the colored trivalent graph G' as simply some extra structure on M.

Lemma 5.4.2. *Let $(M, r, \lambda(\partial M)_1)$ be an extended cobordism from $(\Sigma, \lambda(\Sigma)_1)$ to itself and $(M, r, \lambda(\partial M)_2)$ be an extended cobordism from $(\Sigma, \lambda(\Sigma)_2)$ to itself. Then $Z((M, r, \lambda(\partial M)_1))$ is strong shift equivalent to $Z((M, r, \lambda(\partial M)_2))$.*

Proof. First we notice that

$$\lambda(\partial M)_1 = \lambda(\Sigma)_1 \oplus \lambda(\Sigma)_1 \in H_1(\Sigma) \oplus H_1(\bar{\Sigma}),$$

$$\lambda(\partial M)_2 = \lambda(\Sigma)_2 \oplus \lambda(\Sigma)_2 \in H_1(\Sigma) \oplus H_1(\bar{\Sigma}).$$

Then we have

$$\begin{aligned}
&(M, r, \lambda(\partial M)_1) \\
&= (\Sigma \times I, 0, \lambda(\Sigma)_1 \oplus \lambda(\Sigma)_2) \cup_{(\Sigma, \lambda(\Sigma)_2)} (M, r, \lambda(\Sigma)_2 \oplus \lambda(\Sigma)_1), \\
&(M, r, \lambda(\partial M)_2) \\
&= (M, r, \lambda(\Sigma)_2 \oplus \lambda(\Sigma)_1) \cup_{(\Sigma, \lambda(\Sigma)_1)} (\Sigma \times I, 0, \lambda(\Sigma)_1 \oplus \lambda(\Sigma)_2).
\end{aligned}$$

Here we consider $(M, r, \lambda(\Sigma)_2 \oplus \lambda(\Sigma)_1)$ as a cobordism from $(\Sigma, \lambda(\Sigma)_2)$ to $(\Sigma, \lambda(\Sigma)_1)$. Then by the functoriality of Z, we have the conclusion. □

Lemma 5.4.3. *Suppose we have a closed extended 3-manifold $((M, r), \chi)$ with an infinite cyclic covering. We obtain two extended fundamental domains M_1 and M_2 by slicing along two extended surfaces $(\Sigma, \lambda(\Sigma))$ and $(\Sigma', \lambda(\Sigma'))$ which are dual to χ. We obtain two morphisms*

$$\begin{aligned}
&(M_1, r_1, \lambda(\Sigma) \oplus \lambda(\Sigma)) : (\Sigma, \lambda(\Sigma)) \to (\Sigma, \lambda(\Sigma)), \\
&(M_2, r_2, \lambda(\Sigma') \oplus \lambda(\Sigma')) : (\Sigma', \lambda(\Sigma')) \to (\Sigma', \lambda(\Sigma')),
\end{aligned}$$

with weight r_1, r_2 respectively such that the closures of both cobordism having weight r. Then

$$Z((M_1, r_1, \lambda(\Sigma) \oplus \lambda(\Sigma))) \sim Z((M_2, r_2, \lambda(\Sigma') \oplus \lambda(\Sigma')).$$

Proof. We just need prove the case where Σ and Σ' are disjoint from each other. See [Li6, Proof of Theorem 8.2], [G3]. Since Σ' is disjoint from Σ, we can choose a copy of $(\Sigma', \lambda(\Sigma'))$ inside $(M_1, r_1, \lambda(\Sigma) \oplus \lambda(\Sigma))$. We cut along Σ' and get two 3-manifolds T, S. We assign to T, S extended 3-manifold structures, denoted by $(T, t, \lambda(\Sigma) \oplus \lambda(\Sigma'))$ and $(S, s, \lambda(\Sigma') \oplus \lambda(\Sigma))$, such that if we glue R to S along Σ', we get $(M_1, r_1, \lambda(\Sigma) \oplus \lambda(\Sigma))$ back. We need to choose appropriate weights t, s for T, S. Using Definition 5.2.10, we see that such t, s exists. Now we just need prove that if we glue S to T along Σ, we obtain $(M_2, r_2, \lambda(\Sigma')\oplus\lambda(\Sigma'))$. Actually, it is easy to see that after gluing, we have the right base manifold and lagrangian subspace. What we need to prove is that we get the right weight. This follows from Lemma 5.2.13. $\square$

As a consequence of the two lemmas above, we have the following:

Proposition 5.4.4. *For a tuple $((M, r), \chi)$ and $(M_1, r_1, \lambda(\Sigma_1)\oplus\lambda(\Sigma_1))$ given as in Lemma 5.4.3, the strong shift equivalent class of the map $Z((M_1, r_1, \lambda(\Sigma_1)\oplus\lambda(\Sigma_1)))$ is independent of the choice of the extended surface $(\Sigma_1, \lambda(\Sigma_1))$. Thus we may denote this SSE class by $\mathcal{Z}((M, r), \chi)$.*

Next, we work towards constructing a fundamental domain for an extended 3-manifold $((M, r), \chi)$ with an infinite cyclic covering. Suppose we have a surgery presentation (D_0, L, s) in standard form for $((M, r), \chi)$, here $s = r - \sigma(L)$ [GM2, Lemma(2.2)]. We do 0-surgery along K_0 and get a link L in $(S^2 \times S^1, s)$. We cut $S^2 \times S^1$ along the 2-sphere containing D_0 in this product structure and obtain a tangle T in $(S^2 \times I, s)$ in standard form. Here, we say that a tangle is in standard form if it comes from slicing a surgery presentation diagram in standard form. Then we drill out tunnels along arcs which meet the bottom and glue them back to the corresponding place on the top. We obtain a cobordism $\hat{E}$ from Σ_g to itself with a link $\hat{L}$ embedded in it as in Figure 5.8, where Σ_g is a genus g closed surface. See [G1, Figure 3] for example. Moreover, we identify Σ_g with a standard surface as pictured in Figure 5.9. We denote by $\lambda_{\mathcal{A}}$ the lagrangian subspace spanned by the curves labelled by a_i in Figure 5.9. We assign the lagrangian subspace $\lambda_{\mathcal{A}}$ to each connected component of the boundary of $\hat{E}$. Moreover, we assign the weight s to it. Thus we obtain an extended cobordism $(\hat{E}, s, \lambda_{\mathcal{A}} \oplus \lambda_{\mathcal{A}})$.

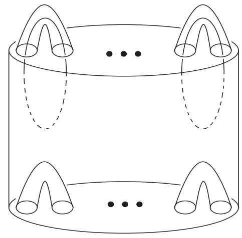

FIGURE 5.8. The extended cobordism $(\hat{E}, s, \lambda_{\mathcal{A}} \oplus \lambda_{\mathcal{A}})$ containing a framed link $\hat{L}$. If we do extended surgery along $\hat{L}$, we get a fundamental domain E. If, instead, we color $\hat{L}$ by ω, we obtain another cobordism E'.

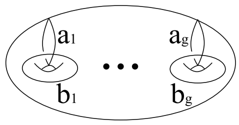

FIGURE 5.9. A surface in standard position.

Proposition 5.4.5. *The closure of* $(\hat{E}, s, \lambda_{\mathcal{A}} \oplus \lambda_{\mathcal{A}})$ *is* $(S^3(U), s, 0)$*, where* U *is a* 0*-framed unknot.*

Proof. It is easy to see that the closure of $\hat{E}$ is $S^3(U)$. Then we just need to prove that the weight of the closure is s. By the gluing formula and Definition 5.2.11, we have that the weight on $S^3(U)$ is

$$s + 0 - \mu(\lambda_E(\Sigma_g \cup \bar{\Sigma}_g), \lambda(\Sigma_g \cup \bar{\Sigma}_g), \lambda_{\Sigma_g \times [0,1]}(\Sigma_g \cup \bar{\Sigma}_g)).$$

Now let

$$H_1(\Sigma_g) = < a_1, \cdots, a_g, b_1, \cdots, b_g >, H_1(\bar{\Sigma}_g) = < a_1', \cdots, a_g', b_1', \cdots, b_g' > .$$

Then

$$\begin{aligned}
\lambda_E(\Sigma_g \cup \bar{\Sigma}_g) &= i^{-1}_{\Sigma_g \cup \bar{\Sigma}_g, E}(0) \\
&= \{(x, y) \mid x \in < a_1, \cdots, a_g >, y \in < b_1', \cdots, b_g' >\}. \\
\lambda_{\Sigma_g \times [0,1]}(\Sigma_g \cup \bar{\Sigma}_g) &= i^{-1}_{\Sigma_g \cup \bar{\Sigma}_g, \Sigma_g \times [0,1]}(0) \\
&= < (a_i, -a_i'), (b_i, -b_i') \mid i = 1, \cdots, g > . \\
\lambda(\Sigma_g \cup \bar{\Sigma}_g) &= \lambda_{\mathcal{A}} \oplus \lambda_{\mathcal{A}} \\
&= \{(x, y) \mid x \in < a_1, \cdots, a_g >, y \in < a_1', \cdots, a_g' >\}
\end{aligned}$$

So

$$
\begin{aligned}
& \lambda(\Sigma_g \cup \bar{\Sigma}_g) + \lambda_E(\Sigma_g \cup \bar{\Sigma}_g) \\
= \; & \{(x,y) \mid x \in < a_1, \cdots, a_g >, y \in < a'_1, \cdots, a'_g > + < b'_1, .., b'_g >\} \\
= \; & \{(x,y) \mid x \in < a_1, \cdots, a_g >, y \in H_1(\bar{\Sigma}_g)\}.
\end{aligned}
$$

Therefore,

$$
\begin{aligned}
& \lambda_{\Sigma_g \times [0,1]}(\Sigma_g \cup \bar{\Sigma}_g) \cap [\lambda(\Sigma_g \cup \bar{\Sigma}_g) + \lambda_E(\Sigma_g \cup \bar{\Sigma}_g)] \\
= \; & < (a_i, -a'_i) \mid i = 1, \cdots, g > .
\end{aligned}
$$

It is easy to see that the bilinear form defined in [Wall] is identically 0 on $< (a_i, -a'_i) \mid i = 1, \cdots, g >$. So we have

$$\mu(\lambda_E(\Sigma_g \cup \bar{\Sigma}_g), \lambda(\Sigma_g \cup \bar{\Sigma}_g), \lambda_{\Sigma_g \times [0,1]}(\Sigma_g \cup \bar{\Sigma}_g)) = 0.$$

Then we get the conclusion. □

Proposition 5.4.6. *Let $(E, s, \lambda_{\mathcal{A}} \oplus \lambda_{\mathcal{A}})$ be the result of extended surgery along the embedded link $\hat{L}$ in $(\hat{E}, s, \lambda_{\mathcal{A}} \oplus \lambda_{\mathcal{A}})$ constructed as above starting with a standard surgery presentation diagram for $((M, r), \chi)$. $(E, s, \lambda_{\mathcal{A}} \oplus \lambda_{\mathcal{A}})$ is a fundamental domain for $((M, r), \chi)$.*

Proof. The closure of $(E, s, \lambda_{\mathcal{A}} \oplus \lambda_{\mathcal{A}})$ can be obtained by performing extended surgery on the closure of $(\hat{E}, s, \lambda_{\mathcal{A}} \oplus \lambda_{\mathcal{A}})$. This uses the commutative property of gluing discussed in [GM2]. Thus the closure of E is diffeomorphic to M, and by [GM2, Lemma 2.2], we see that the closure of $(E, s, \lambda_{\mathcal{A}} \oplus \lambda_{\mathcal{A}})$ has weight r. □

.

Proposition 5.4.7. *Let $(E', s, \lambda_{\mathcal{A}} \oplus \lambda_{\mathcal{A}})$ be the extended cobordism obtained by coloring the link $\hat{L}$ in $(\hat{E}, s, \lambda_{\mathcal{A}} \oplus \lambda_{\mathcal{A}})$ by ω. The SSE class $\mathcal{Z}((M, r), \chi)$ is given by*

$$Z(E', s, \lambda_{\mathcal{A}} \oplus \lambda_{\mathcal{A}}).$$

Proof. The equality $Z(E, s, \lambda_{\mathcal{A}} \oplus \lambda_{\mathcal{A}}) = Z(E', s, \lambda_{\mathcal{A}} \oplus \lambda_{\mathcal{A}})$ follows from the surgery axiom [GM2, Lemma 11.1] for extended surgery. $\square$

5.5 The relation between the Turaev-Viro endomorphism and the tangle endomorphism.

In this section, we will prove the following theorem.

Theorem 5.5.1. *If $((M, r), \chi)$ is an extended 3-manifold with an infinite cyclic covering having a surgery presentation (D_0, L, s) in standard form, then $\mathcal{Z}((M, r), \chi) = Z(D_0, L, s)$.*

Proof. For simplicity, we indicate the proof in case that $((M, r), \chi)$ does not have a colored trivalent graph. The argument may easily be adapted to the more general case.

We obtain a tangle $\hat{L}_n$ from the surgery presentation (D_0, L, s), and we place black dots on segments in the top part. We will directly compute two matrices for these two endomorphisms with respect to some bases.

Step 1: Compute the entry for the Turaev-Viro endomorphism. We will use the basis in [BHMV2] for $V(\Sigma_g)$, where Σ_g is genus g surface. Specifically we choose our spine to be a lollipop graph, as in [GM1]. We show one example of elements as in Figure 5.10.

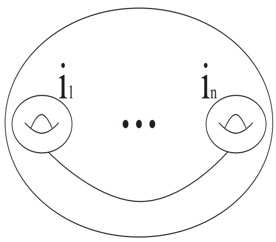

FIGURE 5.10. An example of elements in the basis for $V(\Sigma_g)$ constructed in [BHMV2].

Using the method employed in [G2, §8], we can compute the entries of the matrix, with respect to this basis by computing the quantum invariants of colored links in a connected sum of $S^1 \times S^2$'s . We have

$$\begin{aligned} &(i_1, \cdots, i_g)\text{-}(j_1, \cdots, j_g) \text{ entry of } Z((E', s, \lambda_{\mathcal{A}} \oplus \lambda_{\mathcal{A}}) \\ = &\frac{\eta\kappa^{s-\sigma(L')} < \text{the first diagram in Figure 5.11} >}{\eta\kappa^{-\sigma(L'')} < \text{the first diagram in Figure 5.12} >}. \end{aligned}$$

where L' as in Figure 5.11 and L'' as in Figure 5.12.

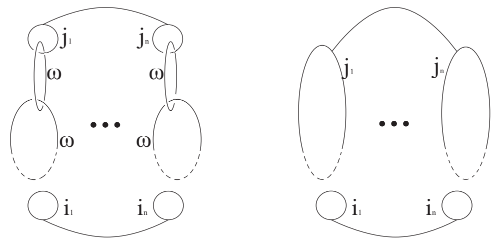

FIGURE 5.11. L' is consisted of components colored with ω.

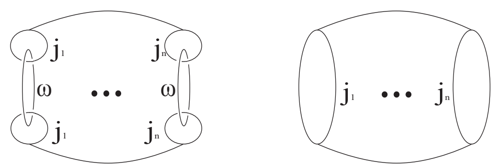

FIGURE 5.12. L'' is consisted of components colored with ω.

By using fusion and Lemma 6 in [Li4] and the fact that

$$\sigma(L') = \sigma(L'') = 0,$$

we have

$$\begin{aligned} &(i_1, \cdots, i_g)\text{-}(j_1, \cdots, j_g) \text{ entry of } Z((E', -\sigma(L), \lambda_{\mathcal{A}} \oplus \lambda_{\mathcal{A}}) \\ = &\frac{\eta\kappa^s\eta^n\Delta_{j_1}\cdots\Delta_{j_n} < U(\omega) >^n < \text{the second diagram in Figure 5.11} >}{\eta < U(\omega) >^n < \text{the second diagram in Figure 5.12} >} \\ = &\frac{\kappa^s\eta^n\Delta_{j_1}\cdots\Delta_{j_n} < \text{the second diagram in Figure 5.11} >}{< \text{the second diagram in Figure 5.12} >} \end{aligned}$$

where $U(\omega)$ is the 0-framing unknot colored with ω.

Step 2: Compute the entry for tangle endomorphism.

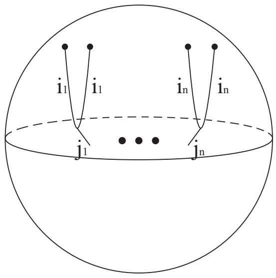

FIGURE 5.13. Elements in a basis for $V(S^2; 2n)$ which do not automatically vanish under $Z(\hat{L}_n)$ have this form.

By gluing the tangle in $(S^2 \times I, s)$ to the basis element in Figure 5.13, we can see that

$$\begin{aligned} & (i_1, \cdots, i_g)\text{-}(j_1, \cdots, j_g) \text{ entry of } Z(\hat{L}_n) \\ = \ & \frac{\kappa^s \eta^n \Delta_{j_1} \cdots \Delta_{j_n} < \text{the second diagram in Figure 5.11} >}{< \text{the second diagram in Figure 5.12} >} \end{aligned}$$

for $(i_1, \cdots, i_n, j_1, \cdots, j_n)$ a legal coloring, and is zero otherwise.

Step 3: The two matrices are strong shift equivalent. By above discussion, it is easy to see that if the matrix for Turaev-Viro endomorphism is X, then a matrix for tangle endomorphism is the block matrix

$$\begin{bmatrix} X & 0 \\ 0 & 0 \end{bmatrix}.$$

We see that this block matrix is strong shift equivalent to X by Proposition 5.2.22.

□

5.6 Proof of Theorem 5.3.7

Lemma 5.6.1. *The transformation process in Proposition 5.2.19 does not change the strong shift equivalent class of the tangle endomorphism.*

Proof. A small extended Kirby-1 move adds a ± 1 framed ω to all the different decorations of $\mathcal{T}_n^n$ which go into the definition of $Z(\mathcal{T}_n^n)$. This would seem to multiply $Z(\mathcal{T}_n^n)$ by $\kappa^{\pm 1}$. But a small extended Kirby-1 move also changes $\sigma(L)$ by

± 1, and thus changes the weight s of $S^2 \times I \supset \mathcal{T}_n^n$ by ∓ 1. These two effects of the move cancel out and $Z(\mathcal{T}_n^n)$ is unchanged. The small Kirby-2 moves preserves all the summands of $Z(\mathcal{T}_n^n)$, by a well known handle slide property of ω. See [KL, Lemma 21] for instance. Two tangles related by a D_0 move are obtained by cutting $S^2 \times S^1$ along two different S^2's. Suppose if we cut $S^2 \times S^1$ along $S_0 = S^2 \times \{p_0\}$, we obtain a tangle $\hat{L}_n$. If we cut along $S_1 = S^2 \times \{p_1\}$, we obtain a tangle $\hat{L}'_m$. By those two cutting, we obtain two homomorphisms

$$Z(\hat{L}_n) : V(S_1) \to V(S_1)$$

and

$$Z(\hat{L}'_m) : V(S_0) \to V(S_0).$$

Now suppose we cut $S^2 \times S^1$ along $S^2 \times \{p_0\}$ and $S^2 \times \{p_1\}$, we get a (n, m)-tangle in $(S^2 \times I, 0)$, denoted by T_1, and a (m, n)-tangle, denoted by T_2. T_1 defines a homomorphism

$$Z(T_1) : V(S_1) \to V(S_0),$$

and T_2 defines a homomorphism

$$Z(T_2) : V(S_0) \to V(S_1).$$

It is easy to see that

$$Z(\hat{L}_n) = Z(T_2)Z(T_1),$$

and

$$Z(\hat{L}'_m) = Z(T_1)Z(T_2).$$

Therefore, $Z(\hat{L}_n)$ is strong shift equivalent to $Z(\hat{L}'_m)$. □

Lemma 5.6.2. *Suppose we have two surgery presentations* (D_0, L_1, s_1, G_1) *and* (D_0, L_2, s_2, G_2) *for* (M, r, χ, G') *in standard form, then*

$$Z(D_0, L_1, s_1, G_1) = Z(D_0, L_2, s_2, G_2).$$

Proof. This easily follows from Propositions 5.5.1. □

Proof of Theorem 5.3.7. By Proposition 5.2.19, and Lemma 5.6.1, we can transform (D_0, L_1, s_1, G_1) and (D_0, L_2, s_2, G_2) so that they are standard without changing the SSE class of their induced tangle endomorphism. Then the result follows from Lemma 5.6.2. □

5.7 Colored Jones polynomials and Turaev-Viro endomorphisms

In this section, we assume, for simplicity, that p is odd. Similar formulas could be given for p even, by the same methods. We let $J(K, i)$ denote the bracket evaluation of a knot diagram of K with zero writhe colored i at a primitive $2p$th root of unity A. Letting U denote the unknot, we have that $J(U, i) = \Delta_i$. In particular, $J(U, 1) = -A^2 - A^{-2}$. This is one normalization of the colored Jones polynomial at a root of unity.

Remark 5.7.1. Using [BHMV1, Lemma 6.3], we have that:

$$J(K, i + p) = -J(K, i), \text{ and } J(K, i + (p - 1)/2) = J(K, -i + (p - 3)/2).$$

Without losing information, we can restrict our attention to $J(K, 2i)$ for $0 \leq i \leq (p-3)/2$. For other c, $J(K, c) = \pm J(K, 2i)$ for some $0 \leq i \leq (p-3)/2$, using the above equations.

Let $(S^3(K), i, j, 0))$ denote 0-framed surgery along an oriented knot K in S^3 decorated with a meridian to K colored i and a longitude little further away from K colored j and equipped with the weight zero. Let χ be the homomorphism from $H_1(M)$ to $\mathbb{Z}$ which sends a meridian to one. Let $\mathrm{TV}(K, i, j)$ denote the SSE class of the Turaev-Viro endomorphism $\mathcal{Z}(S^3(K), i, j, 0)), \chi)$. The vector space associated to a 2-sphere with just one colored point which is colored by an odd number is zero. Using this fact, and a surgery presentation, one sees that

$$\mathrm{TV}(K, i, j) = 0 \text{ if } i \text{ is odd.}$$

The second author studied $\mathrm{TV}(K, i, 0)$ [G1, G2]. The idea of adding the longitude with varying colors is due to Viro [V1, V2]. The least interesting case, of this next theorem, when $j = 0$ already appeared in [G1, Corollary 8.3].

Theorem 5.7.2 (Viro)**.** *For* $0 \leq j \leq p-2$*,*

$$J(K, j) = \sum_{i=0}^{(p-3)/2} \Delta_{2i} \operatorname{Trace}(\mathrm{TV}(K, 2i, j)).$$

Proof. One has that 0-framed surgery along K with the weight zero is the result of extended surgery of S^3 with weight zero along a zero-framed copy of K. If we add then a zero-framed meridian of K to this framed link description, we undo the surgery along K and we get back an extended surgery description of S^3, also with weight zero. A longitude to K colored j and placed a little outside the meridian will go to a longitude of K colored j in S^3, which is of course isotopic to K. But adding a zero-framed meridian to the framed link changes $< \, >_p$ in the same way as cabling by $\omega = \eta \sum_{i=0}^{(p-3)/2} \Delta_{2i} e_{2i}$. If we cable the meridian of K by e_{2i} instead of by ω, and calculate $< \, >_p$, we get

$$< (S^3(K), 2i, j, 0) >_p = \operatorname{Trace}(\mathrm{TV}(K, 2i, j)),$$

by the trace property of TQFT [BHMV2, 1.2]. Thus

$$< S^3 \text{ with } K \text{ colored } j >= \eta \sum_{i=0}^{(p-3)/2} \Delta_{2i} \operatorname{Trace}(\mathrm{TV}(K, 2i, j)).$$

Dividing by η yields the result. $\square$

Thus the colored Jones is determined by the traces of the $\mathrm{TV}(K, 2i, j)$. The next theorem shows that the $J(K, j)$ determine the traces of the $\mathrm{TV}(K, 2i, j)$.

Theorem 5.7.3. *For* $0 \leq i, j \leq (p-3)/2$,

$$\mathrm{Trace}(\mathrm{TV}(K, 2i, 2j)) = \eta^2 \sum_{k=0}^{(p-3)/2} \sum_{l=|k-j|}^{k+j} \Delta_{(2k+1)(2i+1)-1} J(K, 2l).$$

More generally :

$$\mathrm{Trace}(\mathrm{TV}(K, 2i, j)) = \eta^2 \sum_{k=0}^{(p-3)/2} \sum_{\substack{l = |2k-j| \\ l \equiv j \mod 2}}^{2k+j} \Delta_{(2k+1)(2i+1)-1} J(K, l).$$

.

Proof. By the trace property of TQFT,

$$\mathrm{Trace}(\mathrm{TV}(K, 2i, 2j)) =< (S^3(K), 2i, 2j) >_p .$$

Direct calculation of $< (S^3(K), 2i, 2j) >_p$ from the definition yields η times the bracket evaluation of K cabled by ω together with the meridian colored $2i$ and the longitude further out colored $2j$. These skeins all lie in a regular neighborhood of K with framing zero. These skeins can then be expanded as a linear combination of the core of this solid torus with different colors.

The operation of encircling an arc colored $2k$ with loop colored $2j$ in the skein module of a local disk has the same effect as multiplying the arc by $\Delta_{(2k+1)(2j+1)-1}/\Delta_{2k}$ by [Li6, Lemma 14.2]. Note the idempotents f_k are only defined for $0 \leq k \leq (p-2)$. It is well known that the e_k satisfy a recursive formula which can be used to extend the definition of e_k for all $k \geq 0$. This is given [BHMV1] as follows: $e_0 = 1$, e_1 is the zero framed core of a solid standard solid torus, and $e_k = ze_{k-1} - e_{k-2}$. In the skein module of a solid torus, we have $e_{2k}.e_{2j} = \sum_{l=|k-j|}^{k+j} e_{2l}$. Using these rules, the expansion can be worked out to be

$$\eta \sum_{k=0}^{(p-3)/2} \sum_{l=|k-j|}^{k+j} \Delta_{(2k+1)(2i+1)-1} e_{2l}.$$

The second equation is worked out in a similar way. □

Notice that, in the summation on the right of the first equation in Theorem 5.7.3, $J(K, 2l)$ for $l > (p-3)/2$ sometimes appears. This can be rewritten using Remark 5.7.1 as $J(K, 2j)$ for $j \leq (p-3)/2$.

We remark that using [G4, Corollary 2.8], one can see that the Turaev-Viro polynomials of $\mathrm{TV}(K, i, j)$ will have coefficients in a cyclotomic ring of integers, if p is an odd prime or twice an odd prime.

5.8 Examples

In this section, we wish to illustrate with some concrete examples how to calculate the $\mathrm{TV}(K, i, j)$ using tangle morphisms in the case $p = 5$ (which is the first interesting case). For both examples, we check our computation against an identity from the previous section.

The first example is the k-twist knot with meridian colored 0 or 2 and longitude colored 2. We then verify directly the equation in Theorem 5.7.2 for the case $p = 5$, $j = 2$, and K is the k-twist knot.

The second example we study is the knot 6_2 with the meridian and longitude uncolored. We work out, using tangle morphisms, the traces of the Turaev-Viro endomorphism. We then verify the equation in Theorem 5.7.3 when $p = 5$, $i = j = 0$, and $K = 6_2$.

We pick an orthogonal basis for the module associated with a 2-sphere with some points, and use this basis to work out the entries on the matrix for the tangle endomorphism coming from a surgery presentation. The bases are represented by colored trees in the 3-ball which meet the boundary in the colored points as in Figure 5.13. Here we will refer to these colored trees as basis-trees. Each entry is obtained as a certain quotient. The numerator is the evaluation as a colored fat graph in S^3 obtained from the tangle closed off with the source basis-tree at the bottom and the target basis-tree at the top. The denominator is the quotient as the evaluation of the double of the target basis element. In both examples, we use a surgery presentation, with one surgery curve with framing +1. Thus the initial weight of S^3, denoted s above, should be -1, so the weight of S^3 after the surgery is zero. This puts a factor of κ^{-1} in front of the tangle endomorphism. There is also a uniform factor of η coming from the single black dot on a strand with two endpoints. We put this total factor of $\kappa^{-1}\eta$ in front. We also have Δ_i prefactors where i is the color of the strand with the black dot, and these factor vary from entry to entry.

To simplify our formulas, when $p = 5$, we use Tet to abbreviate $\mathrm{Tet}(2, 2, 2, 2, 2, 2)$, Δ to abbreviate $\Delta_1 = \Delta_2$ and Θ to denote $\Theta(2, 2, 2)$.

5.8.1 The Turaev-Viro endomorphism and the colored Jones polynomial of the k-twist knot.

A tangle T for the k-twist knot with meridian and longitude is given in Figure 5.14.

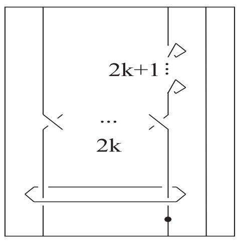

FIGURE 5.14. Surgery presentation of k-twist knot with meridian and longitude. The straight line is from the meridian and the circle is from the longitude. We have also chosen a position for the black dot.

If we denote by T_0 the tangle T with meridian colored by 0 and longitude colored by 2, and let S denote a 2-sphere with two uncolored points, then we obtain a map

$$\mathrm{TV}(K, 0, 2) = Z(T_0) : V(S) \to V(S).$$

By using the trivalent graph basis in [BHMV2],

$$V(S) = \text{Span} < a_1, a_2 >,$$

where a_1, a_2 are as in Figure 5.15. With respect to this basis, we have

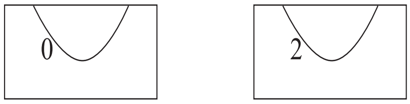

FIGURE 5.15. A basis for $V(S)$ where S is a 2-sphere with two uncolored points

$$\text{TV}(K, 0, 2) = \kappa^{-1}\eta \begin{bmatrix} \Delta & \Delta^3 \\ \Delta A^{16k+8} & \Delta(A^8 + \Delta A^{8k+8}). \end{bmatrix}$$

We follow the convention that the columns of the matrix for a linear transformation with respect to a basis are given the images of that basis written in terms of that basis. The characteristic polynomial of this matrix (i.e. the Turaev-Viro polynomial) has coefficients in $\mathbb{Z}[A]$.

If we denote by T_2 the tangle T with meridian colored by 2 and longitude colored by 2, and let S denote a 2-sphere with two uncolored points and one point colored 2, then we obtain a map

$$\text{TV}(K, 2, 2) = Z(T_2) : V(S) \to V(S).$$

By using the trivalent graph basis in [BHMV2],

$$V(S) = \text{Span} < b_1, b_2, b_3 >,$$

where b_1, b_2, b_3 are as in Figure 5.16.

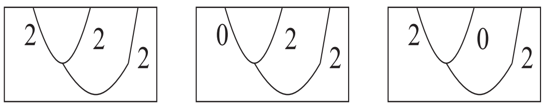

FIGURE 5.16. A basis for $V(S)$ where S is a 2-sphere with two uncolored points and one point colored 2

With respect to this basis, we have

$$TV(K,2,2) = \kappa^{-1}\eta \begin{bmatrix} -(\frac{A^8}{\Delta} + \frac{A^{8k+8}\Delta\,\mathrm{Tet}}{\Theta^2}) & 0 & 0 \\ 0 & 0 & 0 \\ 0 & 0 & 0 \end{bmatrix}.$$

By Proposition 5.2.22, we also have $TV(K,2,2) = \begin{bmatrix} -\kappa^{-1}\eta(\frac{A^8}{\Delta} + \frac{A^{8k+8}\Delta\,\mathrm{Tet}}{\Theta^2}) \end{bmatrix}$. This last expression lies in $\mathbb{Z}[A]$ for all k. One has that:

$$\begin{aligned} & \mathrm{Trace}(TV(K,0,2)) + \Delta\,\mathrm{Trace}(TV(K,2,2)) \\ = \ & \kappa^{-1}\eta\Delta(1 + A^8 + \Delta A^{8k+8}) - \kappa^{-1}\eta\Delta(\frac{A^8}{\Delta} + \frac{A^{8k+8}\Delta\,\mathrm{Tet}}{\Theta^2}). \end{aligned}$$

Moreover, we used recoupling theory as in [MV, KL, Li6] to calculate the 2-colored Jones polynomial of k-twist knot directly to obtain:

$$J(K,2) = -\frac{A^4}{\Delta} + (1 + \frac{\Delta^2\,\mathrm{Tet}}{\Theta^2 A^8})A^{8k}$$

We used Mathematica to verify that the two calculations agree for all k.

5.8.2 The Turaev-Viro endomorphism of 6_2 and quantum invariant of $S^3(6_2)$.

In this section, we will compute the Turaev-Viro endomorphism and quantum invariant of $S^3(6_2)$ when A is a primitive 10th root of unity and verify that the trace of the Turaev-Viro endomorphism equals to quantum invariant. By 6_2, we mean the knot as pictured in [CL], which is the mirror image of the knot as pictured in [Li1, R2]. A tangle T for $S^3(6_2)$ is as in Figure 5.17.

So we obtain a map

$$\mathrm{TV}(6_2, 0, 0) = Z(T) : V(S) \to V(S).$$

where S is a 2-sphere with four uncolored points. We use a trivalent graph basis in [BHMV2] for $V(S)$ as in Figure 5.18.

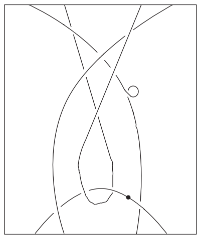

FIGURE 5.17. Tangle for $S^3(6_2)$, with a choice for the position for the black dot.

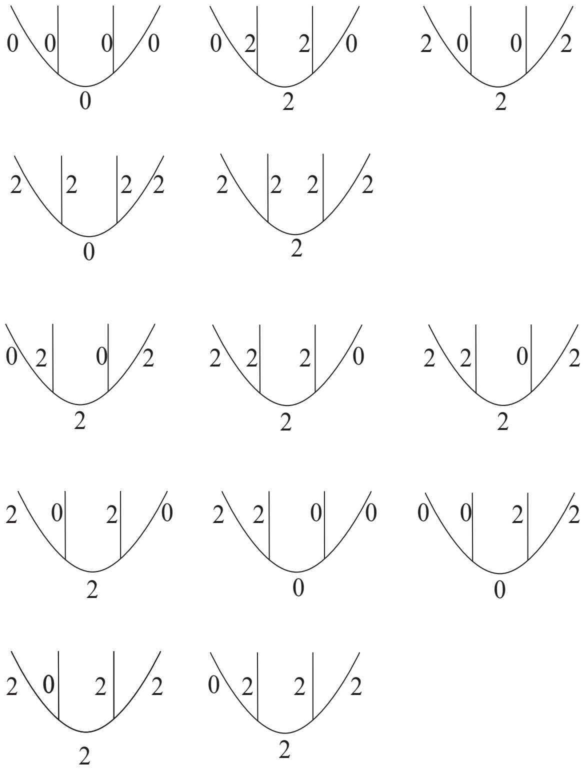

FIGURE 5.18. A basis for $V(S)$, where S is a 2-sphere with four uncolored points.

With respect to this basis, we can obtain a 13×13 matrix, which is in the strong shift equivalence class of the Turaev-Viro endomorphism. However, by Proposition 5.2.22 applied twice in succession, it is enough to consider the minor given by the first five rows and columns. We thus obtain a 5×5 matrix:

$$\mathrm{TV}(6_2, 0, 0) = \kappa^{-1}\eta \begin{pmatrix} 1 & 0 & \Delta^2 & 0 & 0 \\ A^2 & 0 & \Delta(A^3 + A) & 0 & 0 \\ 0 & A^4 & 0 & \Delta & A^2\Theta \\ 0 & \frac{A^8}{\Delta} & 0 & A^8 & \frac{A^8\Theta}{\Delta} \\ 0 & \frac{\Delta A^2}{\Theta} & 0 & \frac{\Delta^2}{\Theta} & \Delta(1 - A^6 + A^8 + \frac{(A^4 - A^6)\Delta\,\mathrm{Tet}}{\Theta^2}) \end{pmatrix}.$$

The Turaev-Viro polynomial (at $p = 5$) is the characteristic polynomial of the above matrix, namely:

$$x^5 + \left(A^3 + A - 1\right) x^4 + \left(-A^3 - A^2 - A\right) x^3 + \left(A^2 + A + 1\right) x^2 + \left(A^3 - A^2 - 1\right) x - A^3.$$

We also note that

$$\mathrm{Trace}(\mathrm{TV}(6_2, 0, 0)) = 1 - A - A^3.$$

The left hand side of the first equation in Theorem 5.7.3, with $i = j = 0$, and $K = 6_2$ is by definition, the quantum invariant of $S^3(6_2)$. The right hand side is, by direct computation:

$$\eta^2(J(6_2, 0)\Delta_0 + J(6_2, 2)\Delta_2 = \eta^2(1 + \Delta(-A^{-2} + A^2 - A^8 - A^6)) = 1 - A - A^3$$

Therefore, we verify a case of the first equation in Theorem 5.7.3.

References

[AB] H. Achir, C. Blanchet, On the computation of the Turaev-Viro module of a knot, Journal Of Knot Theory and Its Ramifications. Vol 7, No. 7 (1998), 843-856.

[A] M. Atiyah, Topological quantum field theories, Inst. Hautes Estudes Sci. Publ. Math, No 68 (1988): 175-186.

[BHMV1] C. Blanchet, N. Habegger, G. Masbaum, P. Vogel, *Three-manifolds invariants derived from the Kauffman bracket*, Topology 31 (1992), 685–699

[BHMV2] C. Blanchet, N. Habegger, G. Masbaum, P. Vogel, Topological quantum field theories derived from the Kauffman bracket. Topology 34 (1995), No. 4, 883-927.

[BH] M.Boyle, D.Handelman, Algebraic shift equivalence and primitive matrices, Trans. Amer. Math. Soc. 336, No. 1 (1993), 121-149.

[BP] D. Bullock, J.H. Przytycki, Multiplicative Structure Of Kauffman Bracket Skein Module Quantizations, Proc. Amer. Math. Soc. Volume 128 (2000), 923-931.

[Cai] X. Cai, A Gram determinant for Lickorish's bilinear form, Math. Proc. Cam. Phil. Soc. 151, issue 01 (2011), 83–94.

[CGT] , X. Cai, P. Gilmer, R. Todd, Mahler measure of colored Jones polynomials, private communication.

[CG] X. Cai, P. Gilmer, On the Turaev-Viro endomorphism and the colored Jones Polynomial, to appear in Algebraic & Geometric Topology.

[CM] , X. Cai, T. Mansour, Bilinear Forms On Skein Modules And Steps In Dyck Paths, J. Math. Phys., Vol. 52 (2011).

[CK] A. Champanerkar, I. Kofman, On the Mahler Measure of Jones Polynomials Under Twisting, Algebraic & Geometric Topology, Volume 5, 2005, pp 1-20.

[CL] J. C. Cha and C. Livingston, KnotInfo: Table of Knot Invariants, http://www.indiana.edu/ knotinfo, January 31, 2012.

[CP] Q. Chen,J. Przytycki, The Gram determinant of the type B Temperley-Lieb algebra, Adv. in Appl. Math. 43 (2009), No. 2, 156-161.

[C] L. Comtet, Advanced combinatorics: The art of finite and infinite expansions, Revised and enlarged edition. D. Reidel Publishing Co., Dordrecht, 1974.

[Co] J.H. Conway, An enumeration of knots and links, and some of their algebraic properties, in Computational problems in abstract algebra, Pergamon (1970), 329-358.

[DGG] P. Di Francesco, O. Golinelli, E. Guitter, Meanders and the Temperley-Lieb algebra, Comm. Math. Phy. 186 (1997), 1-59.

[DiF] P. Di Francesco, Meander determinants, Comm. Math. Phy. 191 (1998), 543–583.

[FGL] C. Frohman, R. Gelca, W. Lofaro, The A-Polynomial From The Noncommutative Viewpoint, Tran. Amer. Math. Soc., Vol. 254 (2001), 735-747.

[G] S. Garoufalidis, Difference and differential equations for the colored Jones function, J. Knot Theory Ramifications 17, No. 4 (2008), 495-510.

[GS] J. Genauer, N. W. Stoltzfus, Explicit diagonalization of the Markov form on the Temperley-Lieb algebra, Math. Proc. Cambridge Philos. Soc. 142 (2007), No. 3, 469-485.

[GM1] P. M. Gilmer, G. Masbaum, Integral Lattices in TQFT, Annales Scientifiques de l'Ecole Normale Superieure, 40, (2007), 815-844

[GM2] P. M. Gilmer, G. Masbaum, Maslov index, lagrangians, mapping class groups and TQFT, arXiv:0912.4706v3. to appear in Forum Mathematicum

[G1] P. M. Gilmer, Invariants for one-dimensional cohomology classes arising from TQFT, Topology And Its Applications 75 (1997), 217-259.

[G2] P. M. Gilmer, Turaev-Viro modules of satellite knots, KNOTS '96, Tokyo, 1996.

[G3] P. M. Gilmer, Topological quantum field theory and strong shift equivalence, Canad. Math. Bull. 42 (1999), 190-197.

[G4] P. M. Gilmer, Integrality for TQFTs, Duke Math. J. 125 (2004) 389-413.

[G5] P. M. Gilmer, Lecture Notes.

[J] V. Jones, A polynomial invariant for knots via Von Newmann algebras, Bulletin AMS, Vol 12, No. 1 (1985), 103-111.

[KL] L. H. Kauffman and S. L. Lins. Temperley-Lieb recoupling theory and invariants of 3-manifolds, volume 134 of Annals of Mathematics Studies. Princeton University Press, 1994.

[Ka1] L. H. Kauffman, State models and the Jones polynomial, Topology 26 (1987), 395-407.

[Ka2] L. Kauffman, Knots in Physics, World Scientific Press 1994.

[K] R. Kirby, A calculus for framed links in S^3, Invent. Math. 45 (1978), No. 1, 35-56.

[KS] K. H. Ko, L. Smolinsky, A combinatorial matrix in 3-manifold theory, Pacific J. Math. 149 (1991), No. 2, 319-336.

[La] W Lawton, A problem of Boyd concerning geometric means of polynomials, J. Number Theory 16 (1983), 356-362.

[L] T. Le, The colored Jones polynomial and the A-polynomial of knots, Adv. Math. 207, No. 2 (2006), 782-804.

[Li1] W. B. R. Lickorish, Three manifolds and the Temperley-Lieb algebra, Math. Ann. 290 (1990), 756-670.

[Li2] W. B. R. Lickorish, Calculations with the Temperley-Lieb algebra, Comm. Math. Helv. 67 (1992), 571-591.

[Li3] W. B. R. Lickorish, Skeins and handlebodies, Pac. J. Math. 159 (1993), 337-349.

[Li4] W. B. R. Lickorish, The skein method for 3-manifold invariants, J. Knot Th. Ram. 2 (1993), 171-194.

[Li5] W. B. R. Lickorish, Invariants for 3-manifolds from the combinatorics of the Jones polynomial. Pac. J. Math. 149 (1991), 337–347.

[Li6] W. B. R. Lickorish, An introduction to knot theory, Graduate Texts in Mathematics, 175. Springer-Verlag, New York, 1997.

[LM] D. Lind, B. Marcus, Introduction to Symbolic Dynamics and Coding, Cambridge University Press 1995.

[MV] G. Masbaum, P. Vogel, 3-valent graphs and the Kauffman bracket, Pacific J. Math. 164 (1994), No. 2, 361-381.

[O1] T. Ohtsuki, Equivariant quantum invariants of the infinite cyclic covers of knot complements, Intelligence of low dimensional topology 2006, 253-262, Ser. Knots Everything 40, World Sci. Publ., Hackensack, NJ, 2007.

[O2] T. Ohtsuki, Invariants of knots derived from equivariant linking matrices of their surgery presentations, Internat. J. Math. 20 (2009), No. 7, 883–913.

[Sk] N. Skoruppa, Heights, Graduate course, Bordeaux (1999), http://wotan.algebra.math.uni-siegen.de/ countnumber/D/

[RT] N. Reshetikhin, V. Turaev, Invariants of 3-manifolds via link polynomials and quantum groups, Invent. Math. 103 (1991), No. 3, 547-597.

[R1] D. Rolfsen, Knots and links, Mathematics Lecture Series, 7. Publish or Perish, Inc., Houston, TX, 1990.

[R2] D. Rolfsen, A surgical view of Alexander's polynomial, Lecture Notes in Math., Vol. 438, Springer, Berlin, 1975.

[TL] N. Temperley and E., Lieb, Relations between the percolation and coloring problem and other graph-theoretical problems associated with regular planar lattices: some exact results for the percolation problem, Proc. Royal Soc. Series A 322 (1971), 251-280.

[T] V. Turaev, Quantum invariants of knots and 3-manifolds, de Gruyter Studies in Mathematics, 18. Walter de Gruyter Co., Berlin, 2010.

[TV] V. Turaev, O. Viro, Lecture by Viro at Conference on Quantum Topology: Kansas State University, Manhattan, Kansas, March 1993

[V1] O. Viro, conversation with P. Gilmer, January 2011

[V2] O. Viro, *Elevating link homology theories and TQFT's via infinite cyclic coverings*, Lecture by Viro at Swiss Knots May 2011, http://www.math.toronto.edu/ drorbn/SK11/

[Wa1] K. Walker, Topological quantum field theories and minimal genus surfaces, Lecture, International Conference on Knots 90, Osaka, Japan, August 1990

[Wa2] K. Walker, On Witten's 3-manifold invariants, Preliminary Version, 1991 http://canyon23.net/math/

[Wag] J. Wagoner, Strong shift equivalence theory and the shift equivalence problem. Bull. Amer. Math. Soc. 36 (1999), no. 3, 271-296.

[Wall] C. Wall, Non-additivity of the signature, Invent. Math. 7 (1969), 269-274.

[Wen] H. Wenzl, On sequence of projections, C. R. Math. Rep. Acad. Sci. IX (1987), 5-25.

[Wilf] H. Wilf, Generatingfunctionology, Academic Press 1990.

[W] E. Witten, Topological quantum field theory, Comm. Math. Phy. 117 (1989): 353-386.

Vita

Xuanting Cai was born in 1984, in Zhuji City, Zhejiang Province, China. He finished his undergraduate studies at Peking University of China in July 2007. In August 2007, he came to Louisiana State University to pursue graduate studies in mathematics. He is currently a candidate for the degree of Doctor of Philosophy in mathematics, which will be awarded in May 2013.